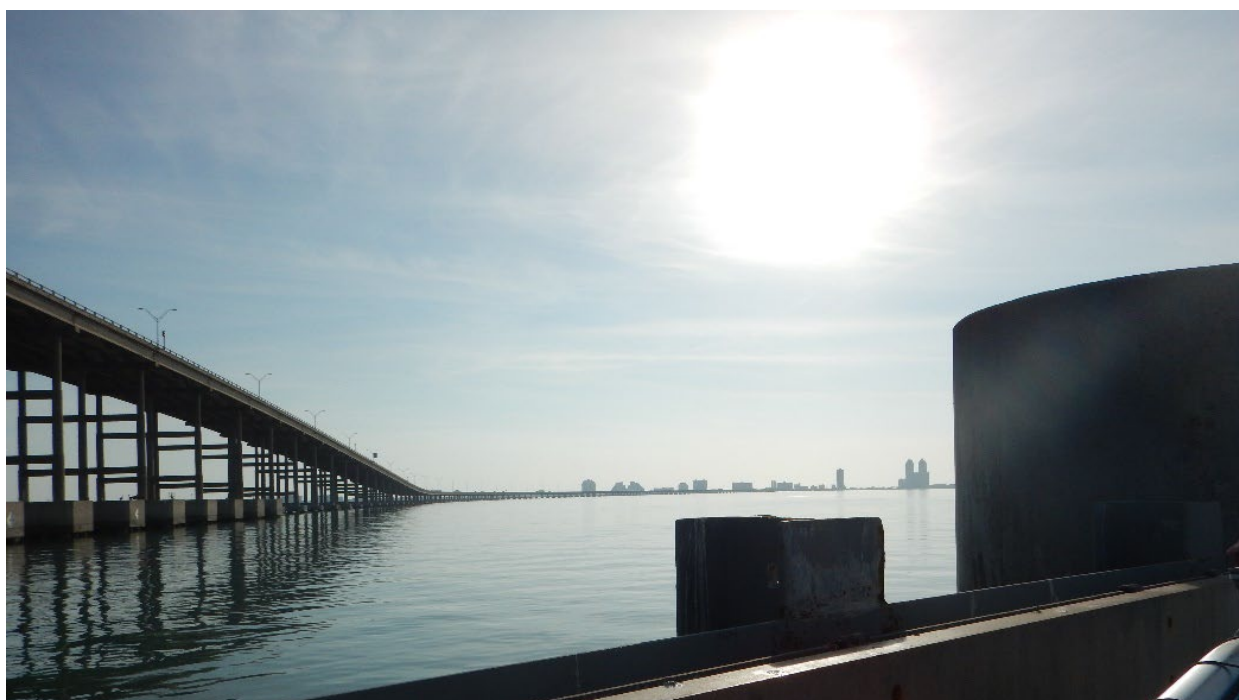


Southwest Texas Current Survey 2017-2019

Aransas Pass to Brazos Santiago Pass



**Silver Spring, Maryland
December 2022**



noaa National Oceanic and Atmospheric Administration

U.S. DEPARTMENT OF COMMERCE
National Ocean Service
Center for Operational Oceanographic Products and Services

Center for Operational Oceanographic Products and Services
National Ocean Service
National Oceanic and Atmospheric Administration
U.S. Department of Commerce

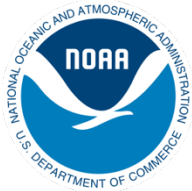
The National Ocean Service (NOS) Center for Operational Oceanographic Products and Services (CO-OPS) provides the National infrastructure, science, and technical expertise to collect and distribute observations and predictions of water levels and currents to ensure safe, efficient and environmentally sound maritime commerce. The Center provides the set of water level and tidal current products required to support NOS' Strategic Plan mission requirements, and to assist in providing operational oceanographic data/products required by NOAA's other strategic plan themes. For example, CO-OPS provides data and products required by the National Weather Service to meet its flood and tsunami warning responsibilities. The Center manages the National Water Level Observation Network (NWLON), a national network of Physical Oceanographic Real-Time Systems (PORTS[®]) in major U.S harbors, and the National Current Observation Program consisting of current surveys in near shore and coastal areas utilizing bottom mounted platforms, subsurface buoys, horizontal sensors and quick response real time buoys. The Center establishes standards for the collection and processing of water level and current data; collects and documents user requirements, which serve as the foundation for all resulting program activities; designs new or improved oceanographic observing systems; designs software to improve CO-OPS' data processing capabilities; maintains and operates oceanographic observing systems; performs operational data analysis/quality control; and produces/disseminates oceanographic products.

Southwest Texas Current Survey 2017-2019

Aransas Pass to Brazos Santiago Pass

Carl Kammerer
Lorraine Heilman
Katie Kirk
Christopher Paternostro

December 2022



U.S. DEPARTMENT OF COMMERCE

Gina M. Raimondo, Secretary

National Oceanic and Atmospheric Administration

Richard Spinrad, Ph.D., Under Secretary of Commerce for Oceans and Atmosphere

National Ocean Service

Nicole LeBoeuf, Assistant Administrator

Center for Operational Oceanographic Products and Services

Richard Edwing, Director

NOTICE

Mention of a commercial company or product does not constitute an endorsement by NOAA. Use of information from this publication for publicity or advertising purposes concerning proprietary products or the tests of such products is not authorized.

TABLE OF CONTENTS

TABLE OF CONTENTS	5
LIST OF FIGURES	6
LIST OF TABLES	8
EXECUTIVE SUMMARY	9
1. INTRODUCTION	10
2. PROJECT DESCRIPTION	11
2.1. Geographic scope	14
2.2. Physical oceanographic overview of the region	15
2.2.1. Corpus Christi Bay	15
2.2.2. Laguna Madre and the Brazos Santiago Pass	16
3. METHODS	17
3.1. Description of instrumentation and platforms	17
3.2. Bottom mounts	18
3.3. ATON.....	20
3.4. Horizontal mount	21
3.5. ADCP setup and data collection	23
3.6. Description of data processing and quality control.....	25
4. DATA ACQUIRED	27
5. STATION RESULTS	28
5.1. STX1801 – Lydia Ann Channel, South End.....	29
5.2. STX1802 – Murray Shoal	34
5.3. STX1813 – Intracoastal Waterway Light 69	39
5.4. STX1814 – Queen Isabella Causeway Bridge.....	44
5.5. STX1820 – Brazos Santiago Pass Entrance.....	48
5.6. STX1821 – Brazos Santiago Pass (SPIP)	53
5.7. STX1822 – Port Isabel Channel, North End.....	57
6. SPATIAL VARIATION	62
6.1. Harmonic constituents.....	62
6.2. Near-surface flows of the tidal current (timing and speed).....	67
7. SUMMARY	70
8. ACKNOWLEDGMENTS	71
9. REFERENCES	72
Appendix A. Station Listing	73
Appendix B. Station Platform Types	75
ACRONYMS	876

LIST OF FIGURES

Figure 2-1. Map of stations occupied during the 2017-2919 survey.	12
Figure 2-2. AIS tracks over the general survey area with survey locations shown.	13
Figure 2-3. Project geographic scope with insets for Corpus Christi Bay (middle) and the Port Isabel region (lower).	15
Figure 3-1. The Research Vessel (R/V) Rossby Wave in Southwest Texas, 2018.	17
Figure 3-2. Clamparatus before adding tube and instrument.	20
Figure 3-3. Side-looking Nortek Aquadopp ready for installation at the end of the pole to be clamped to a fixed structure.	21
Figure 3-4. I-Beam attached to a pier with solar panels and white electronics enclosure box.	22
Figure 3-5. Horizontal crib count on the Queen Isabella Bridge. An acoustic Doppler current profiler (ADCP) is held at the bottom of the pole, below the surface.	23
Figure 5-1. Map of stations discussed in this section (labeled and with red squares) with additional stations with good data (grey circles).	28
Figure 5-2. Scatter plot of north-versus-east velocity for station STX1801 at the prediction bin, bin 5 at 0.9 m below mean lower low water (MLLW).	30
Figure 5-3. Comparison of observed major axis velocity data (green points) to predicted tidal velocity along the major axis for station STX1801. The lower figure shows the non-tidal residual, which is the difference between the predicted and observed velocity from the upper panel.	31
Figure 5-4. STX1801 mean velocity profile by depth. Only depths that passed quality control criteria are shown. This station was configured to collect 0.5 m-bins.	32
Figure 5-5. STX1801 maximum flood current (MFC) timing (Greenwich Intervals [GI] - in red squares) and speed (blue circles) by depth bin.	33
Figure 5-6. STX1801 maximum ebb current (MEC) timing (Greenwich Intervals [GI] - in red squares) and speed (blue circles) by depth bin.	34
Figure 5-7. Scatter plot of north-versus-east velocity for station STX1802 at the prediction bin, bin 5 at 1.2 m below MLLW.	35
Figure 5-8. Comparison of observed major axis velocity data (green points) to predicted tidal velocity along the major axis for station STX1802. The lower figure shows the non-tidal residual, which is the difference between the predicted and observed velocity from the upper prediction bin.	36
Figure 5-9. STX1802 mean velocity profile by depth. Only depths that passed quality control criteria are shown. This station was configured to collect 0.5-m bins.	37
Figure 5-10. STX1802 MFC timing (GI - in red squares) and speed (blue circles) by depth bin.	38
Figure 5-11. STX1802 MEC timing (GI - in red squares) and speed (blue circles) by depth bin.	39
Figure 5-12. Scatter plot of north-versus-east velocity for station STX1813 at the near-surface bin, bin 3 at 1.2 m below MLLW.	40
Figure 5-13. Comparison of observed major axis velocity data (green points) to predicted tidal velocity along the major axis for station STX1813. The lower figure shows the non-tidal residual, which is the difference between the predicted and observed velocity from the upper panel.	41
Figure 5-14. STX1813 mean velocity profile by depth. Only depths that passed quality control criteria are shown. This station was configured to collect 0.5-m bins.	42
Figure 5-15. STX1813 MFC timing (GI - in red squares) and speed (blue circles) by depth bin.	43
Figure 5-16. STX1813 MEC timing (GI - in red squares) and speed (blue circles) by depth bin.	44

Figure 5-17. Scatter plot of north-versus-east velocity for station STX1814 at the center of the channel 28.5 m from the sensor.	45
Figure 5-18. Comparison of observed major axis velocity data (green points) to predicted tidal velocity along the major axis for station STX1814. The lower figure shows the non-tidal residual, which is the difference between the predicted and observed velocity from the upper panel.	46
Figure 5-19. STX1814 mean velocity profile by distance bin. Only distances that passed quality control criteria are shown. This station was configured to collect 2.0-m bins.	47
Figure 5-20. STX1814 MFC timing (GI - in red squares) and speed (blue circles) by distance bin.	47
Figure 5-21. STX1814 MEC timing (GI - in red squares) and speed (blue circles) by distance bin.	48
Figure 5-22. Scatter plot of north-versus-east velocity for station STX1820 at the near-surface bin, bin 9 at 1.8 m below MLLW.	49
Figure 5-23. Comparison of observed major axis velocity data (green points) to predicted tidal velocity along the major axis for station STX1820. The lower figure shows the non-tidal residual, which is the difference between the predicted and observed velocity from the upper panel.	50
Figure 5-24. STX1820 mean velocity profile by depth. Only depths that passed quality control criteria are shown. This station was configured to collect 1.0-m bins.	51
Figure 5-25. STX1820 MFC timing (GI – red squares) and speed (blue circles) by depth bin.	52
Figure 5-26. STX1820 MEC timing (GI – red squares) and speed (blue circles) by depth bin.	53
Figure 5-27. Scatter plot of north-versus-east velocity for station STX1821 at bin 29 (the prediction bin).	54
Figure 5-28. Comparison of observed major axis velocity data (green points) to predicted tidal velocity along the major axis for station STX1821. The lower figure shows the non-tidal residual, which is the difference between the predicted and observed velocity from the upper panel.	55
Figure 5-29. STX1821 mean velocity profile by distance. This station was configured to collect 4.0-m bins.	56
Figure 5-30. STX1821 MFC timing (GI - in red squares) and speed (blue circles) by depth bin.	56
Figure 5-31. STX1821 MFC timing (GI - in red squares) and speed (blue circles) by distance bin. The change in GI timing from bin 1 to bin 2 is due to crossing the maximum GI threshold of 12.42 hours. The GI time for bin 1 is 12.37, and 0.15 for bin 2.	57
Figure 5-32. Scatter plot of north-versus-east velocity for station STX1822 at bin 13 (the prediction bin)	58
Figure 5-33. Comparison of observed major axis velocity data (green points) to predicted tidal velocity along the major axis for station STX1822. The lower figure shows the non-tidal residual, which is the difference between the predicted and observed velocity from the upper panel.	59
Figure 5-34. STX1822 mean velocity profile by distance. This station was configured to collect 2.0 m bins.	60
Figure 5-35. STX1822 MFC timing (GI - in red squares) and speed (blue circles) by distance bin.	60
Figure 5-36. STX1822 MEC timing (GI - in red squares) and speed (blue circles) by distance bin.	61
Figure 6-1. Defant ratios for survey stations. Neither strict semidiurnal tides (Defant ratio <0.25) nor mixed-mainly semidiurnal tides (0.25 to 1.5) were found in the study area. Mixed mainly diurnal tides (>1.5 to <3.0) dominate in the lower Laguna Madre. The entrance to Corpus	

Christi had both mixed- mainly diurnal and predominately diurnal stations (Defant ratio >3.0).....	63
Figure 6-2. M ₂ Tidal ellipses for prediction stations in the entire study region, showing the topographic steering of the ellipses.....	64
Figure 6-3. S ₂ tidal ellipses for prediction stations in the entire study region. Note that these are on a different scale than M ₂ in order to see the ellipses. These data are at a different scale than the M ₂ data.....	65
Figure 6-4. O ₁ tidal ellipses for prediction stations in the entire study region. Note that these are on a different scale than M ₂ in order to see the ellipses. These data are at a different scale than the M ₂ data.....	66
Figure 6-5. K ₁ tidal ellipses for the entire study region. Note that these are on a different scale than M ₂ in order to see the ellipses. These data are at ¼ the scale of the M ₂ data.	67
Figure 6-6. Mean values for the tidal currents during maximum flood and ebb at all stations in the survey.....	68
69	
Figure 6-7. GI timing of maximum flood (top) and ebb (bottom) at all stations in the survey. Note that the colors represent hours from 0 to 12.42 with the end interval limits having the same colors to represent the cyclical tides.	69

LIST OF TABLES

Table 3-1. Platform configurations.....	19
---	----

APPENDICES

Table A-1. Station location and deployment information. Stations not recovered (italicized) do not have a recovery date.....	74
Table B-1. Platform and sensor information for recovered stations, including first bin distance and number of good bins.	75

EXECUTIVE SUMMARY

The National Oceanic and Atmospheric Administration (NOAA) National Ocean Service (NOS) Center for Operational Oceanographic Products and Services (CO-OPS) works to promote safe navigation throughout the U.S. waterways. As part of this effort, the CO-OPS National Current Observation Program (NCOP) acquires, archives, and disseminates information on tidal currents in the coastal U.S., which is used to update the NOAA tidal current predictions. NCOP conducts internal assessments of locations in need of new tidal current predictions. The inside waters of the southwestern Gulf Coast of Texas were identified through this process, as well as through a request from the Brazos Santiago Pilots Association. Tidal current data are collected at new locations to help increase spatial coverage in tidal current observations and predictions and also through revisits to historical stations to update the observations and predictions with increased quality and accuracy. The data products generated are utilized by NOAA and the user community to help ensure safe navigation, make informed coastal zone management decisions, and support the protection of life and property. Furthermore, data collected can be used to inform the development of new hydrodynamic models or provide validation to existing ones.

This report summarizes the data collection and analysis completed by NCOP in the 2017-2019 Southwest Texas (STX) Current Survey. A total of 22 stations were installed for at least 1 lunar month. Currents were measured at each station with an acoustic Doppler current profiler (ADCP) moored with a configuration determined by factors such as station depth, seafloor composition, expected maritime activities, anticipated currents, and available inventory. Concurrent with each deployment and recovery of an ADCP, a vertical conductivity-temperature-depth (CTD) profile was taken to ascertain the physical properties of the seawater at the approximate location of each station.

Each ADCP was configured to collect data in evenly spaced ensembles of averaged velocity observations. These ensembles were typically 6 minutes, but longer durations were used at some locations for power conservation or internal memory limitations. Of the 22 stations, 3 were not recovered (STX1805 [ICW– Corpus Christi Bay, Northern Entrance], STX1809 [ICW– Port Mansfield], and STX1810 [Port Mansfield Entrance Channel]). Nineteen stations collected data of sufficient quality to be analyzed. These data include vertical or horizontal current profiles (speed and direction), water temperature, pressure, and additional quality control variables. Currents were analyzed for tidal constituents using harmonic analysis of the velocity time series data collected by the ADCP. Two stations (STX1816 [Port Isabel Channel] and STX1822 [Port Isabel Channel, North End]) were in proximity, and only STX1822 was used for predictions. Tidal current predictions for each station were made available online via the CO-OPS Tides and Currents website (NOAA, 2021a).

1. INTRODUCTION

The National Ocean Service (NOS) Center for Operational Oceanographic Products and Services (CO-OPS) manages the National Current Observation Program (NCOP). The program's main goal is to improve the quality and accuracy of tidal current predictions. Improving this information is a critical part of NOS' efforts toward promoting safe navigation in our nation's waterways. Mariners require accurate and dependable information on the movement of the waters in which they navigate. As increasingly larger ships utilize our ports and as seagoing commerce continues to increase, there is an increased risk to safe navigation in the nation's ports (NOAA, 2018). CO-OPS acquires, archives, and disseminates information on tides and tidal currents in U.S. ports and estuaries, a vital NOS function since the 1840s. The main source of this information for the public is the CO-OPS Tides and Currents website (NOAA, 2021a). The National Oceanic and Atmospheric Administration (NOAA) previously published hard copy Tidal Current Tables annually as required by the Navigation and Safety Regulations section of the U.S. Code of Federal Regulations (33CFR§164.33). NOAA discontinued the production of these hard copy tables in 2020 due to changes in carriage requirements as set forth by the U. S. Coast Guard (2016), and the predictions are now digitally available and accessible by NOAA. Both the collection and analysis of current observations as well as the dissemination of the data fall under the authority of the Navigation and Navigable Waters title of the U.S. Code (33USC§883a-b).

The flow dynamics of an estuary or tidal river can be modified by changes in natural factors, such as land motion and other morphologic changes, or through man-made alterations, such as the deepening of channels by dredging, harbor construction, bridge construction, the deposition of dredge materials, and the diversion of river flow. Changes in water flow and tidal dynamics can affect the accuracy of tidal current predictions; therefore, new data must be collected periodically to ensure that predictions remain reliable and to adjust them when necessary.

CO-OPS has developed expertise in deploying current profilers throughout the nation's coastal waters via the NCOP program. These data are used for a number of products. In addition to updating existing tidal current predictions and establishing new tidal current prediction locations (Fanelli et al., 2014), data collected through this program are utilized by NOAA and the user community in the production and refinement of other products, such as the validation of hydrodynamic forecast systems (Lanerolle et al., 2011) and integration into commercial navigation software. These products are used to ensure safe navigation, make informed coastal zone management decisions, and protect life and property.

The data described in this report were collected by NCOP during a survey from 2017-2019. A total of 22 stations were occupied for at least 1 lunar month. Of the 22 stations, 19 produced time series of good quality data of sufficient length (generally >29 days) to perform harmonic analysis and generate tidal current predictions or to classify the currents as weak and variable. Three stations were not recovered. Data collected typically contained 6-minute time series of vertical or horizontal current profiles (speed and direction), water temperature, pressure, and additional quality control variables, such as echo intensity and correlation magnitude. The collected data were analyzed, and reports were generated detailing statistical and harmonic analyses to ensure high-quality tidal current predictions. Although the analyses were done on all 19 stations that had data of sufficient quality, there were 5 stations that were weak and variable and 1 station was not-tidal. All data and analysis reports presented herein are available on the Tides and Currents website (NOAA, 2021a) or by contacting the CO-OPS Stakeholder Services Branch (NOAA, 2021b).

2. PROJECT DESCRIPTION

Southwest Texas (STX) was requested to be surveyed by the Brazos Santiago Pilots Association, and was identified by internal assessments within CO-OPS as a top 25 high-priority location for an NCOP current observation project using modern acoustic Doppler current profilers (ADCPs). This was the first large-scale current survey for this region of Southwest Texas. Only the northernmost portion of the survey area at Aransas Pass had historical observations and predictions.

Site locations were proposed based upon the internal needs and capabilities of NOAA, as well as from meetings with users including professional mariners; federal, state, and local partners; and academics and researchers. The locations were finalized based on oceanographic needs, engineering restrictions, and criteria set forth by the International Hydrographic Organization (IHO S-44 §4.5). Figure 2-1 shows a graphic of the stations occupied during this survey. As an example of the type of information used for site selection, Figure 2-2 is overlaid with automatic identification system (AIS) ship tracks to demonstrate that ship track density is a key factor for selecting stations.

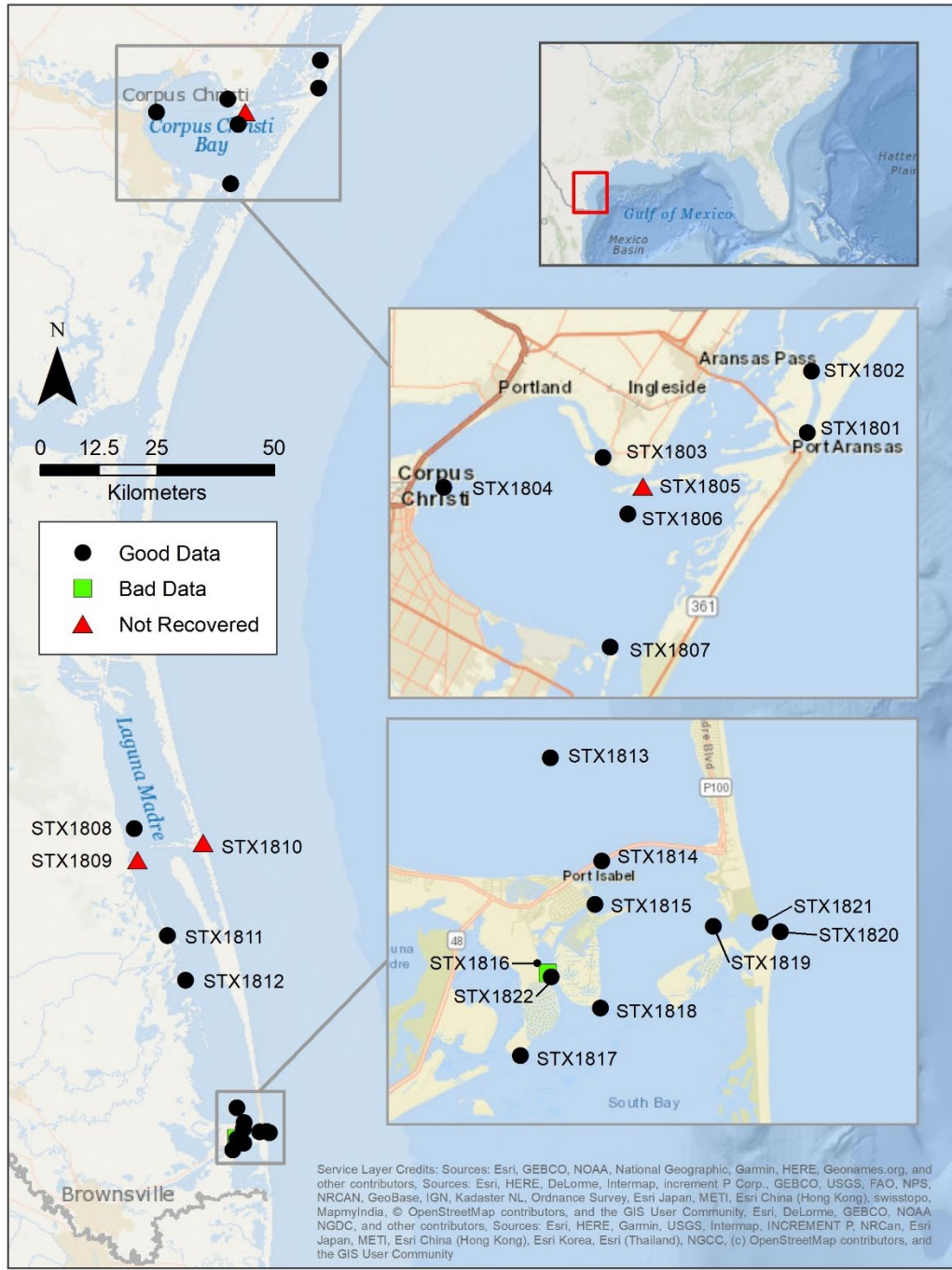


Figure 2-1. Map of stations occupied during the 2017-2919 survey.

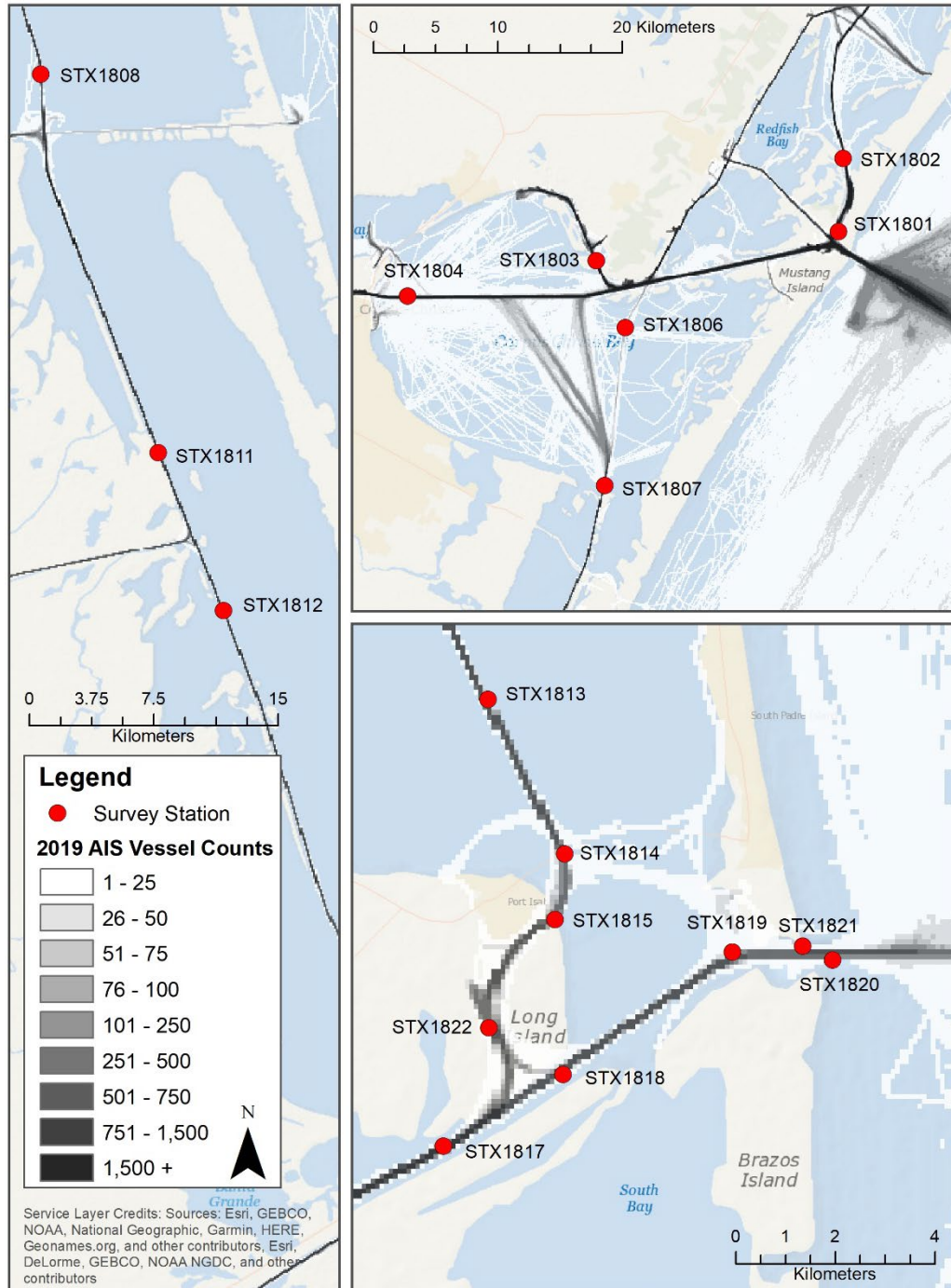


Figure 2-2. AIS tracks over the general survey area with survey locations shown.

In 2015, a field reconnaissance was conducted to gather information about the physical characteristics of the proposed sites. These reconnaissance cruises provided the necessary information for exact locations, platform engineering, and instrument frequencies for the proposed stations. All proposed sites were visited to gather data about their physical characteristics such as depth, bottom type, and vertical profiles of water temperature and salinity. This information was then used to plan the platform and sensor configurations for each current observation station. During reconnaissance

operations, each site was visited using a vessel equipped with a fathometer to determine the depth of the site, a conductivity-temperature-depth (CTD) sensor to determine salinity and water temperature, and a Ponar-style bottom sampler to determine the nature of the seabed at the site (e.g., mud, silt, sand). Based upon the reconnaissance, 21 deployment locations were identified. At the start of operations, 1 station was moved (STX1816 [Port Isabel Channel]) due to damage at the pier at the original location. This station collected data which passed quality control (QC) checks, but was not representative of the channel as needed. Once the original location was repaired, a station was added at the original location (STX1822 [Port Isabel Channel, North End]). The 22 stations were occupied using methods described in Section 3. This technical report focuses on the results of these current profiler deployments.

2.1. Geographic scope

This project collected measurements on inside waters of the southwestern portion of the Texas Gulf Coast, from Aransas Pass to Brazos Santiago Pass (Figure 2-3). This region consisted of 2 distinct sub-regions: Corpus Christi Bay (2.1.1.) and the southern half of Laguna Madre (2.1.2), which includes the adjacent channels near Port Isabel, including the seaward end of the navigational channel to Brownsville.

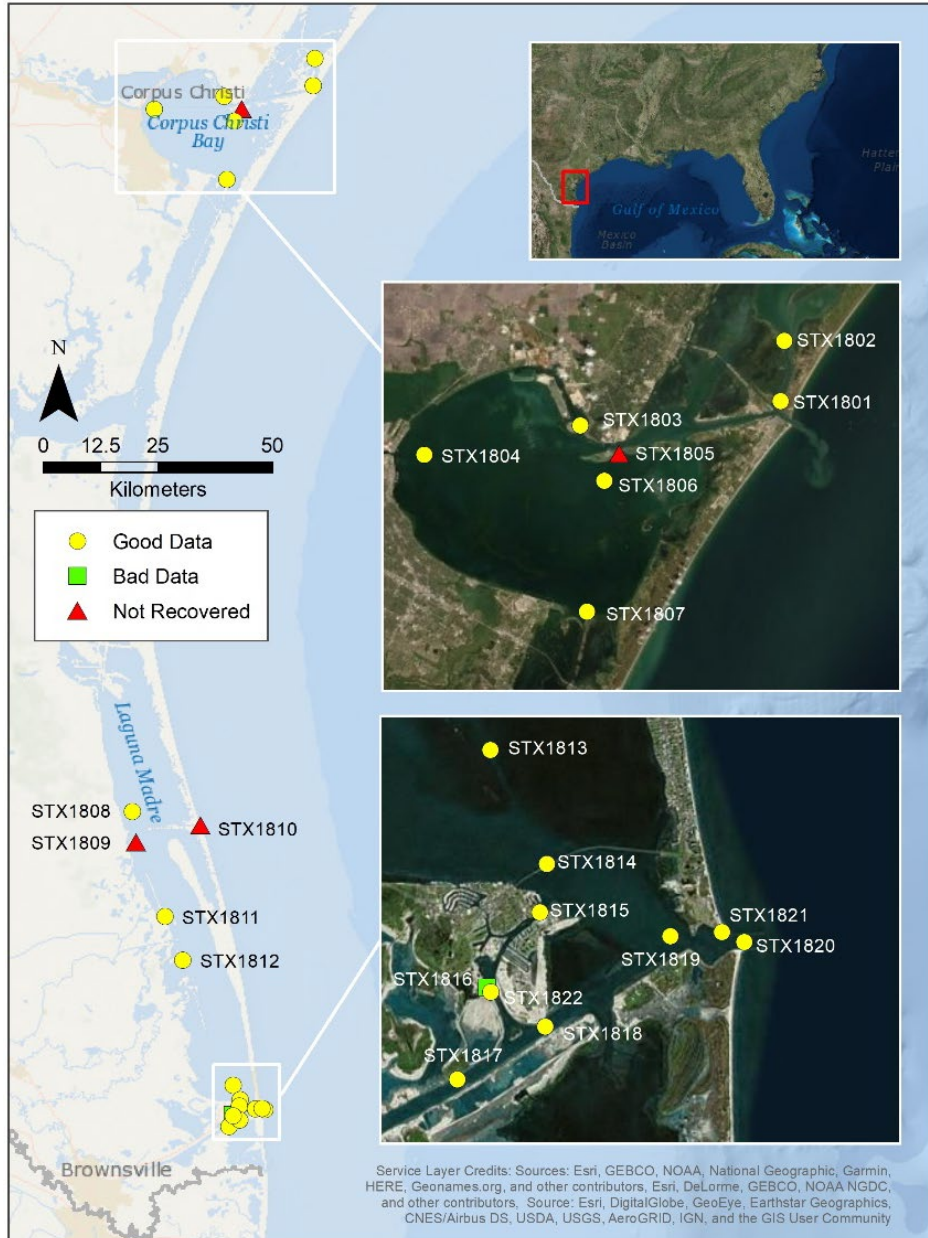


Figure 2-3. Project geographic scope with insets for Corpus Christi Bay (middle) and the Port Isabel region (lower).

2.2. Physical oceanographic overview of the region

2.2.1 Corpus Christi Bay

Situated between Mustang Island and the Texas mainland, Corpus Christi Bay is connected to Nueces Bay to the west and Oso Bay to the southwest, which collectively make up the Nueces Estuary with a combined surface area of about 430 square kilometers (km²) (Texas Water Development Board 2021a). The estuary has average depths of 2.4-4.0 meters (m) (NOAA, 2021d) with deeper shipping channels and the Gulf Intracoastal Waterway (GIWW) and is connected directly to the Gulf of Mexico through the Aransas Pass. It is also connected to the northern portion of the Laguna Madre, via the GIWW to the south and Redfish and Aransas bays to the north, and receives fresh water from the

Nueces River and Oso Creek (Schoenbaechler, et al., 2011a). Tides within the bay are relatively small and mostly, if not strictly, diurnal. Near Corpus Christi (USS Lexington, NOAA tide station ID: 8775296), the great diurnal range (Gt), which is the difference between mean higher high and mean lower low waters, was 0.185 m with a Defant ratio of 5.61. Port Aransas (NOAA tide station ID:8775237) had a larger Gt of 0.318 m and Defant ratio of 2.94 (NOAA, 2021c). The Defant ratio is the ratio of the principal diurnal constituents (O_1 , and K_1) to the principal semidiurnal constituents (M_2 and S_2) of the tides for the major axis and is defined as: $(K_1 + O_1) / (M_2 + S_2)$. This ratio is used to determine the nature of the tide as it changes from strict semidiurnal to strict diurnal: for a Defant ratio less than 0.25, the tides are semidiurnal; for a Defant ratio between 0.25 and 1.5, the tides are mixed, primarily semidiurnal; for a ratio between 1.5 and 3, the tides are mixed but mostly diurnal; and for a ratio greater than 3, the tides are diurnal (Defant, 1958).

2.2.2 Laguna Madre and the Brazos Santiago Pass

Situated between the Texas mainland and the 113-mile-long barrier island of Padre and South Padre barrier islands, the Laguna Madre has a surface area of about 1607 km² and is very shallow with depths of less than 3 m except in maintained channels. The estuary is only connected directly to the Gulf of Mexico through the Port Mansfield Channel near its midpoint and the Brazos Santiago Pass at its southern end (NOAA, 2021d; Texas Water Development Board 2021b). The Brazos Santiago Pass is the more significant of the 2 connections and is the seaward navigation entrance to the ports of Brownsville and Port Isabel. Due to the lack of significant freshwater sources, including rainfall, and high evaporation, there is on average a negative net freshwater inflow to Laguna Madre (Schoenbaechler et al., 2011b), and thus the estuary has higher than normal salinity (hypersalinity). The Upper Laguna Madre (northern portion of the estuary) is non-tidal with only the solar semidiurnal constituent (SSa) consistently having an amplitude in excess of 0.1 m (Gill et al., 1995). Tides in the Lower Laguna Madre near Brazos Santiago Pass are small and strictly diurnal. South Padre Island, Coast Guard Station, (NOAA tide station ID:8779748) has a Gt of 0.416 and a Defant ratio of 3.68. Station SPI Brazos Santiago (NOAA tide station ID:8779749), which is co-located with survey station STX1821 – Brazos Santiago Pass Single Pile Instrumentation Platform (SPIP), has a Gt of 0.449 and Defant ratio of 3.45. Finally, Port Isabel (NOAA tide station ID:8779770) has a Gt of 0.418 and a Defant ratio of 3.25 (NOAA 2021c).

3. METHODS

3.1. Description of instrumentation and platforms

Due to the shallow bathymetry of the region, all on-water operations were conducted on the Research Vessel (R/V) Rossby Wave, a 5.8-m center console catamaran manufactured by Twin Vee (Figure 3.1). These operations consisted of deploying a calibrated ADCP in an appropriate platform at each station location, and recovering it after the planned station occupation period (Table A-1). For each station deployment and recovery, the water depth from the vessel's fathometer was recorded and a CTD vertical profile was taken using a SonTek (previously YSI) CastAway[®] CTD to ascertain the physical properties of the seawater at the approximate location of each station. All station metadata were recorded on station log sheets. For each station, the ADCP instrument's internal compass was calibrated after the batteries were installed. Calibrations were performed to manufacturers' specifications either before the deployment for bottom mounted ADCPs or after the instrument was mounted to the side of an aid to navigation (ATON) for mounted ADCPs. No compass calibrations were conducted on side-looking ADCPs, as they collect data relative to the direction of the instrument (X-Axis, Y-Axis, Z-Axis, [XYZ]) and not in Earth-coordinates (East, North, Up [ENU]). However, detailed directional measurements were made to determine the orientation of side-looking ADCPs relative to Earth.



Figure 3-1. The Research Vessel (R/V) Rossby Wave in Southwest Texas, 2018.




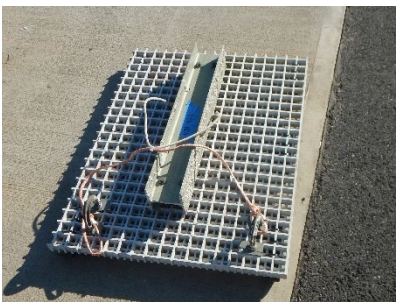
Currents were measured at each station using a moored ADCP with a platform configuration determined by factors such as station depth, seafloor composition, expected maritime activities, anticipated currents, and available instrument and platform inventory. Stations were equipped with one of the following: a Teledyne RD Instruments (TRDI) Workhorse Sentinel with frequencies of 300 kilohertz (kHz), 600 kHz, or 1200 kHz; a Nortek Aquadopp (AqD) with frequencies of 1 megahertz

(MHz) or 2 MHz; a horizontally-facing Nortek (600 kHz); a 2D AqD, 455 kHz Continental; or a 400 kHz acoustic wave and current profiler (AWAC). The maximum distance of an ADCP profile is a function of the instrument frequency, with lower frequency instruments capable of longer profiles. The instrument frequency for each station was therefore determined primarily by anticipated platform depth below the surface at mean higher high water (MHHW) plus an added range buffer to account for uncertainties in depth and potential significant events. At each station, the ADCP was mounted in either a bottom-mounted platform for upward-facing measurements, on a floating ATON for downward-facing measurements, or attached to a fixed structure for horizontal-facing measurements (Table B-1).

3.2. Bottom mounts

Bottom mounts are designed to rest on the seafloor and provide a stable platform for an upward-facing ADCP during station occupation. All bottom-mounted platforms were positioned on the seafloor with no surface presence and were recovered by activating an acoustic release. In the event that the acoustic release failed to work properly, a secondary means of recovery (such as dragging or the use of divers) was employed. Bottom-mount platform configurations used during this project were either manufactured by DeepWater[®] Buoyancy (trawl-resistant bottom mount [TRBM]) or by Mooring Systems Inc. (MSI; miniaturized-TRBM (MTRBM), and ES-2). Table 3-1 provides general specifications, as well as deployment and recovery methods, for each platform.

Table 3-1. Platform configurations

Platform	Specifications	Deployment and Recovery Method	Picture of Platform
MTRBM	<p>Base: 2.5-cm fiberglass grate Shell: Fiberglass or urethane cover with gimbals. Length: 178 cm Width: 122 cm Height: 48 cm Weight in water (without ballast): 23 kg Weight in air: 60 kg</p>	<p>Platform is lowered to place and released. Recovery is by acoustically releasing a float to the surface with a line tethered to the base.</p>	 <p><small>Standard MTRBM system manufactured by MSI</small></p>
Tri-Pod MSI	<p>Aluminum with molded urethane gimbals, lead ballast and stainless-steel hardware. Diameter: 150 cm Height: 50 cm Ballasted Weight air: 31 kg water: 25 kg</p>	<p>Platform is lowered to place and released with a slip line. A ground line is attached between the platform and a small anchor or to a fixed structure. Recovery is with grapnel to snag the ground line.</p>	 <p><small>2019 06 2</small></p>
H-TRBM (Formerly GP35) MSI	<p>Diameter: 89 cm Height: 43 cm 27 kg ballast is used. Weight in seawater: 5 kg (empty) 31 kg (ballasted) Weight in air: 18 kg (empty) 45 kg (ballasted):</p>	<p>Platform is lowered to place and released with a slip line. A ground line is attached between the platform and a small anchor or to a fixed structure. Recovery is with grapnel to snag the ground line.</p>	
Fiberglass Grate NOAA	<p>2.5-cm grid size fiberglass with lead weights as feet and for ballast 45 cm x 55 cm Strong back is used to hold instrument. No gimbal is present.</p>	<p>Platform is lowered to place and released with a slip line. A ground line is attached between the platform and a small anchor or to a fixed structure. Recovery is with grapnel to snag the ground line.</p>	

3.3. ATON

ATON mounted ADCPs are able to observe currents in or adjacent to navigational channels where bottom mounts are impractical or not allowed. For NCOP operations, an Oceanscience Clamparatus (Bosley et al., 2005) without a topside electronics enclosure (Figure 3-) was mounted to the U.S. Coast Guard buoy through an eye bolt which held a downward-facing ADCP in a tube about 2 m below the surface, similar to how a horizontal AqD is mounted (**Error! Reference source not found.**3). A communications cable was attached to the ADCP and fed through the Clamparatus tube for calibration and programming. The cable was left attached and tucked into the tube during the deployment. The ADCP was calibrated on the ATON during deployment to ensure the metal buoy did not interfere with the ADCP compass and magnetic variation. Instruments were configured to collect data internally.



Figure 3-2. Clamparatus before adding tube and instrument.



Figure 3-3. Side-looking Nortek Aquadopp ready for installation at the end of the pole to be clamped to a fixed structure.

3.4. Horizontal mount

Horizontal ADCPs were attached to a fixed structure using either a sled on an I-beam (Figure 3-4), or pole mounted by a clamp (Figure 3-5). The ADCP (AqD 2D; **Error! Reference source not found.**) was oriented to collect data across the channel.



Figure 3-4. I-Beam attached to a pier with solar panels and white electronics enclosure box.



Figure 3-5. Horizontal crib count on the Queen Isabella Bridge. An acoustic Doppler current profiler (ADCP) is held at the bottom of the pole, below the surface.

3.5. ADCP setup and data collection

ADCPs compute water velocity by sending out a series of acoustic pulses, or pings, and measuring each acoustic ping's return signal for Doppler shift. Unlike single-point current meters, ADCPs are generally configured to measure a profile of the water column. Profiles are created from many discrete bins of data collected in the water directly away from the acoustic heads of the ADCP. Bins are determined from the timing of acoustic returns of the unique signal (ping) sent from the instrument transducer using the speed of sound in water to calculate the 2-way travel time over the

distance traveled. Water velocity is calculated by measuring the Doppler shift of each ping after reflection off microscopic bubbles or particulate matter suspended in the water averaged across each bin of the profile.

Bins therefore represent spatially averaged subdivisions along the profile. Optimal bin size is a compromise between higher spatial resolution along the profile (i.e., smaller bins) and lower standard deviation of the velocity ensemble (i.e., larger bin size increases the number of returning pings to calculate the spatial average). Bin size, like profile distance, is also a function of ADCP frequency. Higher frequency instruments measure smaller bins than low frequency instruments with the same standard deviation; however, lower frequency instruments can measure longer profiles and thus are used at deeper stations.

Velocity profiles can be collected either vertically (upward- and downward-facing ADCPs) or horizontally (side-looking ADCPs). Because the ADCP is measuring either a 3-dimensional (bottom and ATON platforms) or 2-dimensional (side-looking) flow field, the acoustic transducer heads are set at an angle with respect to the instrument's measurement profile. For the upward-facing ADCPs used in this survey, the angle is either 20 degrees or 25 degrees. For 3-dimensional flow measurements, a minimum of 3 acoustic transducers are necessary. The Doppler-shifted velocities along each beam can then be transformed mathematically into any orthogonal coordinate system, such as an ENU orientation (with the help of a compass).

Each ADCP was configured to collect profiles of data in 6-minute averages (called "ensembles") of acoustic pulses ("pings"). The pings per ensemble (the number of transmitted acoustic pulses whose returns as described above are averaged in time to form a single velocity measurement for each bin) should minimize the theoretical standard deviation of expected velocity within an ensemble with respect to the engineering constraints of the system. NCOP uses manufacturer-supplied software which calculates the ensemble standard deviation, battery usage, and memory usage for the anticipated duration of the deployment for a specified number of pings per ensemble, number of bins, and bin size. All these factors affect battery life.

The optimal number of pings is a compromise between reducing the ensemble standard deviation and choosing an appropriate bin size and number of bins to ensure sufficient battery life and data storage for the expected conditions at each station. TRDI Workhorses are self-contained ADCPs with internal data storage and battery packs. For this project, stations were configured to minimize standard deviation by maximizing pings per ensemble while still ensuring sufficient battery life to complete the planned deployment duration.

There are some additional constraints on velocity profiles from ADCPs. Because of the angled beams, a portion of the water column near the water surface (or bottom) will be lost to side-lobe interference, (approximately 5-10% of the profile depth depending upon beam angle). Transducer ringing — the result of the noise of the transmit pulse on the co-located transducer and receiver — leads to the loss of part of the profile nearest the ADCP head. Blanking distance accounts for this and varies as a function of ADCP frequency and transducer properties. The manufacturer's recommended default settings for blanking distance were used on both TRDI and Nortek instruments.

In bottom-mounted platforms, the ADCPs have an upward orientation; thus, bin 1 is the bin closest to the ADCP near the seafloor, and the profile extends to the surface. Conversely, in ATON mounts, the ADCP has a downward orientation where bin 1 is near the surface and increases in number with depth. Horizontal ADCPs profile from the instrument outward, where bin 1 is closest to the instrument and increases in number with distance.

The following ancillary measurements were collected and used as data quality assurance parameters: water temperature, pressure (depth), and instrument tilt collected at the sensor. Beam

echo intensity and correlation magnitude were also collected (for TRDI ADCPs only) for each transducer head at each bin of the profile.

ADCPs were calibrated and tested for proper operation using built-in internal testing algorithms. Upon completion of these procedures, a unique configuration file was uploaded to each instrument based upon settings derived from the manufacturers' software. A unique, 5-character deployment name and time to start pinging were also programmed. For all instruments that were redeployed for the second half of the survey, an examination of the ADCP's performance was conducted, and new settings were configured based upon the new location.

3.6. Description of data processing and quality control

The sampling rate for the ADCP data was 10 times per hour (centered every 6 minutes from the top of the hour through 54 minutes past the hour). Each sample was an average of up to 360 evenly timed pings based on the ADCP setup and frequency. Even though the shortest tidal constituent period is about 2 hours, 6-minute samples are frequent enough to enable a high-resolution estimation of the maximum and minimum tidal currents and the ability to capture short duration non-tidal events. This rate also provides a statistically sound time series in which erroneous records are less likely to influence the longer series.

Quality control measures were used to mark each record as bad, good, or questionable based on best practices implemented by CO-OPS (Paternostro et al., 2005) and based on the community-accepted Quality Assurance/Quality Control of Real-Time Oceanographic Data (QARTOD) standards and recommendations (U.S. Integrated Ocean Observing System, 2019 and 2020). Quality controls applied to the measurements consist of threshold checks (for speed, tilt [pitch and roll], echo amplitude, and correlation magnitude, as well as rate of change checks [for speed, pitch, roll, and heading]). An automated algorithm flagged the records that failed any of these thresholds. Questionable data were reviewed by an experienced analyst and marked as either bad or good. Only good data are disseminated to the public and used for harmonic analysis.

The principal flow direction is calculated by maximizing the direction of variance. This calculation enables an orthogonal transformation from an east-north coordinate system to major and minor flow direction axes (generally along- and cross-channel, respectively). Representing the currents in the major and minor axes components is especially beneficial in coastal and estuarine areas, which exhibit a rectilinear reversing flow rather than a rotary flow. In these cases, a significant majority of energy is along the major axis, and we can effectively represent the tidal currents with a single variable (major axis current speed).

All ADCP data collected were analyzed to separate the harmonic or tidal part of the signal from the residual or non-tidal flow (Parker, 2007). Data were extracted from the binary instrument output into columnar ASCII data and then were processed further by NOAA's harmonic analysis routines (Zervas, 1999). Harmonic analyses were then performed upon the current velocity time series in the major and minor flow directions.

The preferred analysis method for tidal current data is an optimization technique called Least Squares Harmonic Analysis (LSQHA) (Parker, 2007). The least squares technique allows for the presence of data gaps and can be used on time series of varying lengths. Amplitudes and phases of a given set of tidal constituents are resolved by using this method. The frequencies and number of tidal constituents for each station are determined by the length of the time series. The least squares method was used to calculate harmonic constituents at all South Texas stations that had good data. We typically collect at least 33 days of data to ensure that most tidal energy can be adequately resolved by

the least squares analysis. Tidal current predictions provided online by CO-OPS are derived directly from these harmonic constituents and meet U.S. Coast Guard vessel carriage requirements.

4. DATA ACQUIRED

Data were acquired at 19 of 22 stations deployed between 2017 and 2019. Three stations were not recovered. Stations STX1805 (ICW - CC Bay Northern Entrance) and STX1809 (ICW Port Mansfield, 1.5 nmi S. of) were adjacent to fixed navigation aids (day boards) that were destroyed by ship strikes and replaced with temporary buoys. Searches were conducted on both stations, but neither instrument was found. The line to station STX1810 parted, and subsequent attempts to recover using divers were unsuccessful.

The estimated depth of the current profiler platform and the measurement bin depths are given in meters relative to an approximation of mean lower low water (MLLW). This approximated MLLW depth is calculated statistically from the known height of the platform above the bottom in combination with the time series from the ADCP's pressure sensor. Since no comparisons are made with nearby water level stations, these approximations may have significant errors. Error in the MLLW calculated at a given current station is the result of both the length of time of observations and uncertainties in the observed station depth. Station depth uncertainty is affected by any pressure sensor errors (such as drift and offset errors) and platform instability. MLLW calculations from observations at water level stations with time series of 30-90 days have, on average, between 4.9 cm and 5.9 cm of uncertainty (NOAA, 2003). Calculated depth is therefore a best approximation. This MLLW approximation can be compared to the station depth, which is logged using the boat's fathometer during deployment and recovery, and entered into the database.

Stations in Table A-1 of appendix A are listed with position, depth as recorded at deployment, and station occupation start and end dates.

5. STATION RESULTS

A brief, quantitative description of a subset of survey stations is provided in this section. These include representative stations that exhibit characteristics of different flow regimes. A map of the stations described in this section is shown in Figure 5-1.

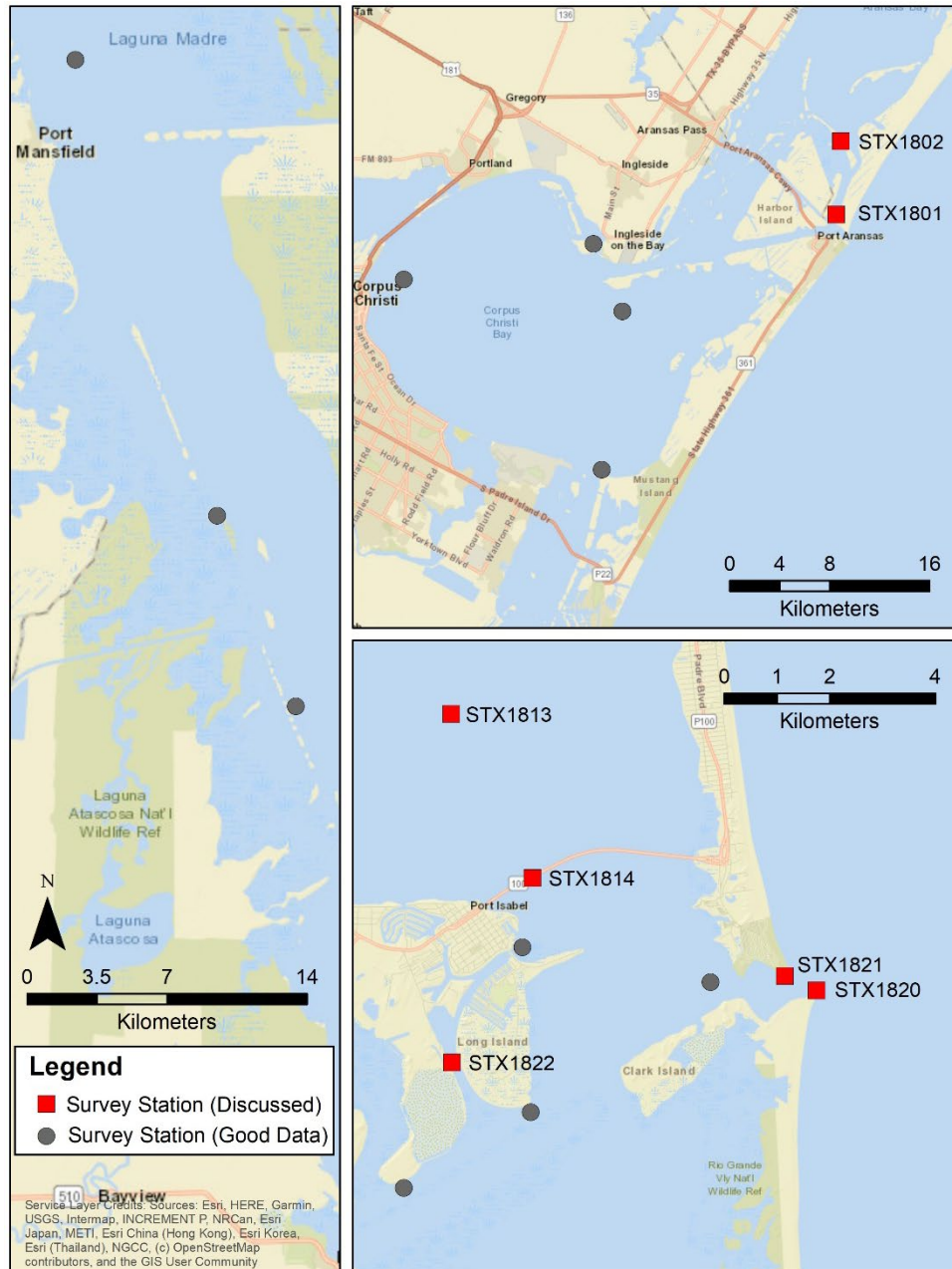


Figure 5-1. Map of stations discussed in this section (labeled and with red squares) with additional stations with good data (gray circles).

For each station in this section, a description of the mean maximum flood current (MFC) and mean maximum ebb current (MEC) is given for the station's prediction bin represented in the official

NOAA tidal current predictions (TCP; NOAA, 2021a). Station STX1820 (Brazos Santiago Pass Entrance) has 3 TCP bins; however, only the surface-most bin is discussed in this section. For ADCPs, bin 1 refers to the depth closest to the instrument's head (bottom-most for bottom mounted, upper-most for ATON-mounted, and closest to the structure for side-looking); the bin number increases with distance from the instrument. The principal flood direction is the predominant axis of flow as described in section 3.6. Directions are provided in degrees from true north. The variance along this axis is provided to give an indication of how confined the flow is along the axis; a high percentage variance implies a rectilinear flow. Seven stations are described in this section. These stations were selected based on spatial representation and/or scientific interest. The results presented below are a small subset of the full analyses conducted on the data sets. Defant ratios for the uppermost bin in the water column or the bin closest to the ship channel are provided to indicate tide type. For each of the 7 stations described, there are 5 figures that include the following:

1. A scatter plot of the north versus east velocity component of the entire dataset at the near-surface depth bin.
2. Two plots of a subset of the velocity time series at the near-surface depth bin; the upper plot shows a comparison of observed (green dots) major-axis velocity and the calculated (red line) tidal predicted velocity; the lower plot shows the residual flow (the difference between observed and predicted velocity).
3. A vertical profile of the mean velocity along the major (red "×") and minor (blue "+") axis of the water column; this represents the approximate mean residual (non-tidal) circulation throughout the water column. The surface level is estimated (shown as a blue wavy line).
4. A vertical profile plot showing the timing and speed of MFC throughout the water column.
5. A vertical profile plot showing the timing and speed of the MEC throughout the water column.

5.1. STX1801 – Lydia Ann Channel, South End

This station was deployed for 60 days (December 01, 2018-January 30, 2019) in 4.5 m (14.8 ft) of water. A TRDI Workhorse 1200 kHz ADCP mounted in a Tripod collected 25 half-meter bins of data, 6 of which met quality control criteria for full analysis. Bin 5 is available as a station on TCP, representing an approximate depth of 0.9 m (3.1 ft.) below MLLW.

Lydia Ann Channel connects Aransas Bay to Corpus Christi Channel and Aransas Pass. Observed currents are rectilinear (Figure 5-2), with major axis variance between 96.2% and 98.7%. This station is mostly tidal, which is indicated by the total accounted energy, as seen in Figure 5-3. The mean flow is greatest near the surface and is reduced slightly with depth (Figure 5-4). LSQHA resolved 24 constituents and accounted for 66-70% of the total energy in the velocity data. Mean MFC and MEC speeds range from 23.1-62.7 centimeters per second (cm/s) (0.5-1.1 knots [kn]). MFC timing indicates a 6-hour jump between near-surface and mid-water bins. This may be due to the suppression of flood currents from the mean southwesterly (ebb) current. MEC were consistent in timing throughout the water column. The Defant ratio in the upper good bin was 2.95, indicating that this station is mixed but almost entirely diurnal.

Julian Days: 335.75-30.94

Velocity North/East - "STX1801-Bin-5"

Orientation: up

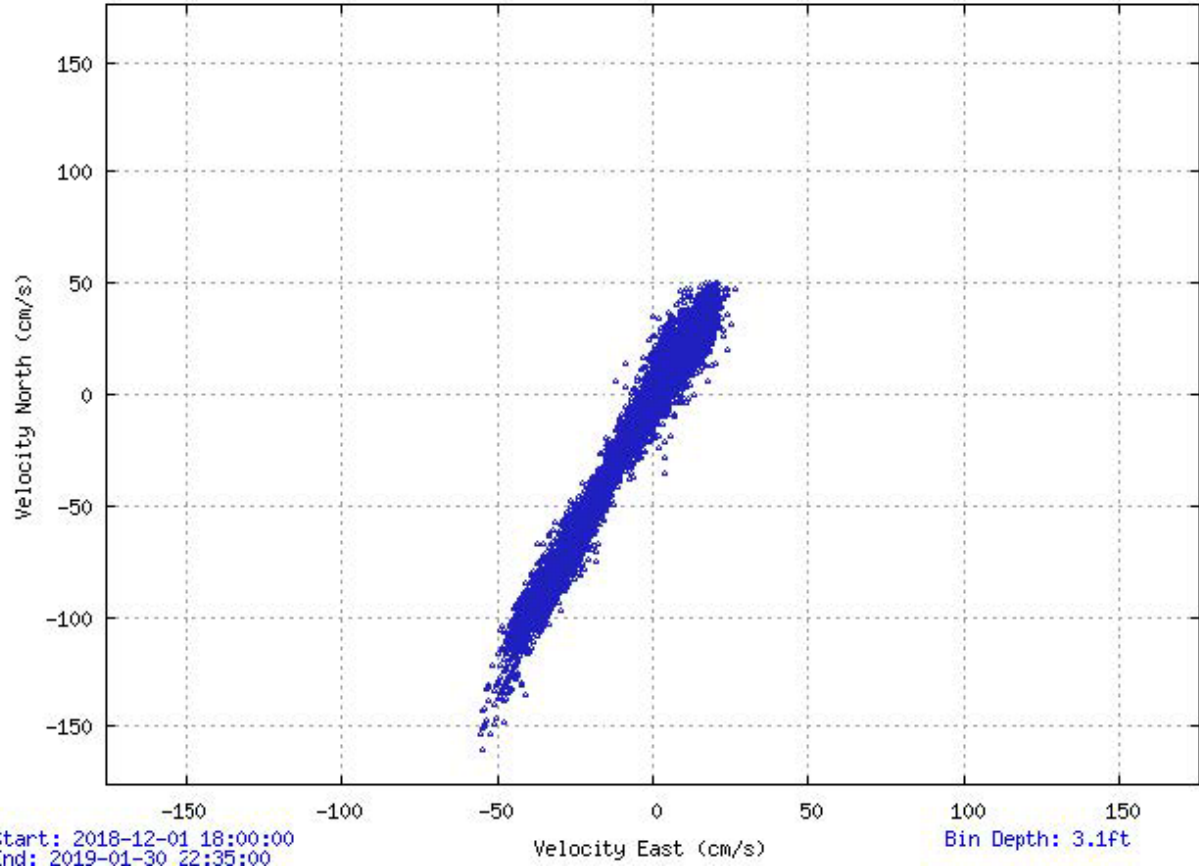


Figure 5-2. Scatter plot of north-versus-east velocity for station STX1801 at the prediction bin, bin 5 at 0.9 m below mean lower low water (MLLW).

Julian Days: 363.76-2.92

Orientation: up

Analysis: LSQHA

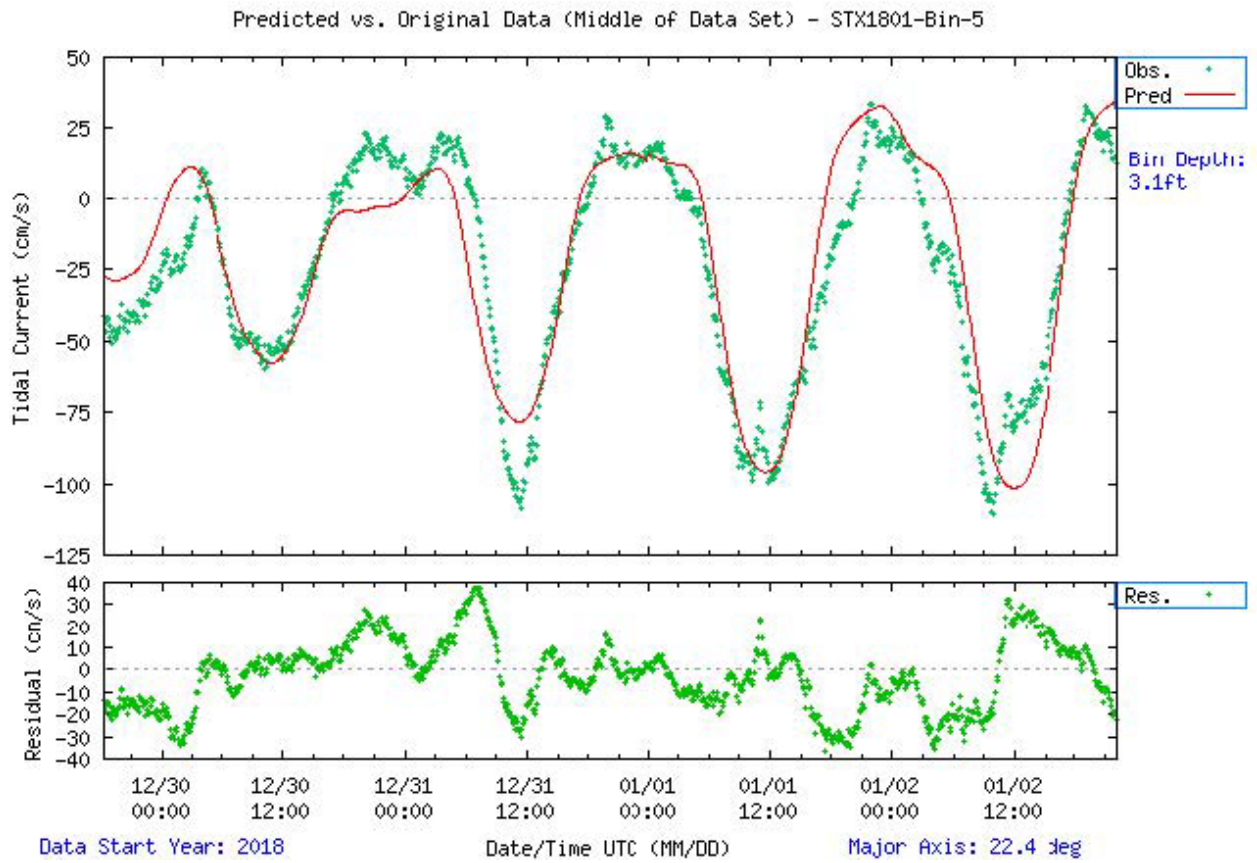


Figure 5-3. Comparison of observed major axis velocity data (green points) to predicted tidal velocity along the major axis for station STX1801. The lower figure shows the non-tidal residual, which is the difference between the predicted and observed velocity from the upper panel.

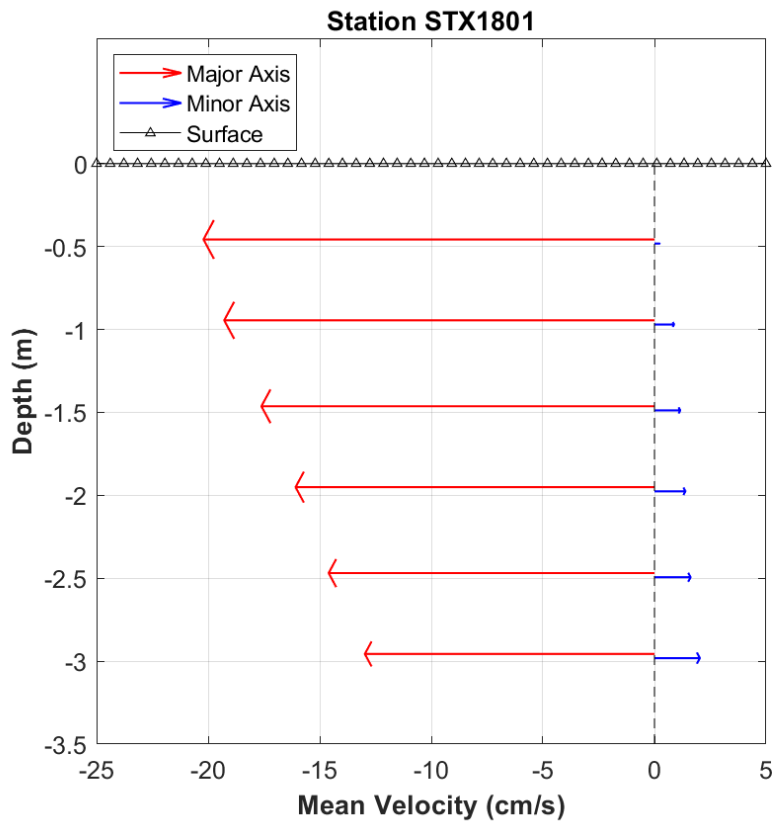


Figure 5-4. STX1801 mean velocity profile by depth. Only depths that passed quality control criteria are shown. This station was configured to collect 0.5 m-bins.

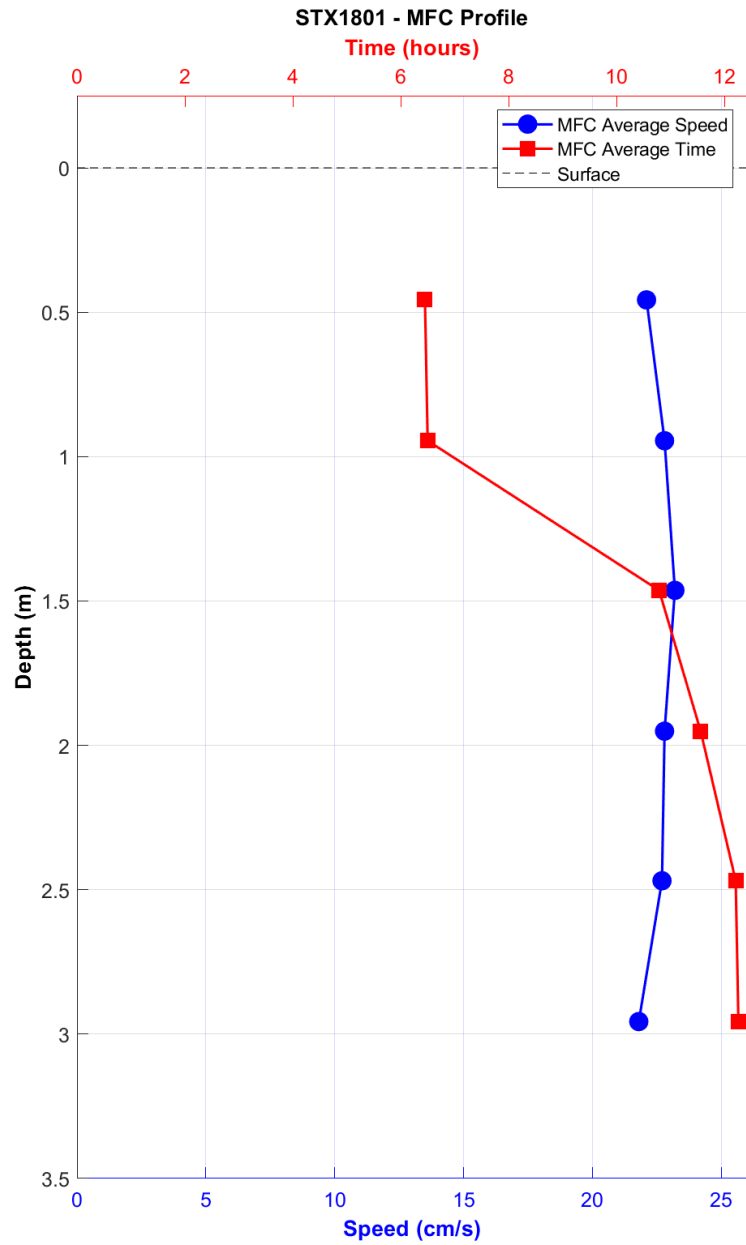


Figure 5-5. STX1801 maximum flood current (MFC) timing (Greenwich Intervals [GI] - in red squares) and speed (blue circles) by depth bin.

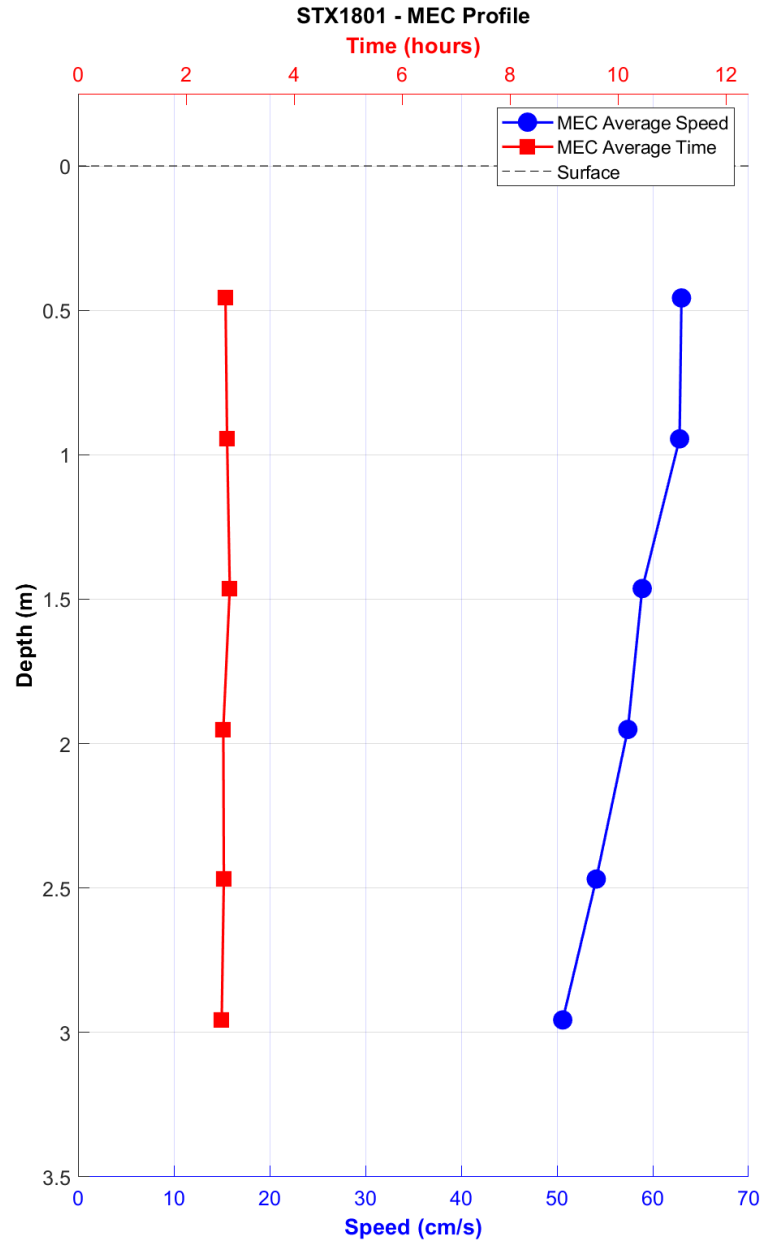


Figure 5-6. STX1801 maximum ebb current (MEC) timing (Greenwich Intervals [GI] - in red squares) and speed (blue circles) by depth bin.

5.2. STX1802 – Murray Shoal

This station was deployed for 59 days (December 01, 2018–January 29, 2019) in 4.0 m (13.1 ft) of water. A 2 MHz Nortek AqD with a 90° head mounted onto a fiberglass grate collected 20 half-meter bins, 6 of which met quality control criteria for full analysis. Bin 5 is available as a station on TCP, representing an approximate depth of 1.2 m (3.9 ft) below MLLW.

Murray Shoal is at the southern end of Aransas Bay where it meets Lydia Ann Channel. Observed currents are rectilinear (Figure 5-7), with major axis variance between 98.9 and 99.5%. This station is mostly tidal, which is indicated by the total accounted energy, as seen in Figure 5-8. A small mean southerly (ebb) current is seen throughout the water column, with maximum speeds mid-depth

(Figure 5-9). LSQHA resolved 25 constituents and accounted for 71-74% of the total energy in the velocity data. Mean MFC and MEC speeds range from 41.6-57.1 cm/s (0.8-1.1 kn), and their timing does not vary much with depth (Figures 5-10 and 5-11). The Defant ratio in the upper good bin was 3.37, indicating that this station is diurnal.

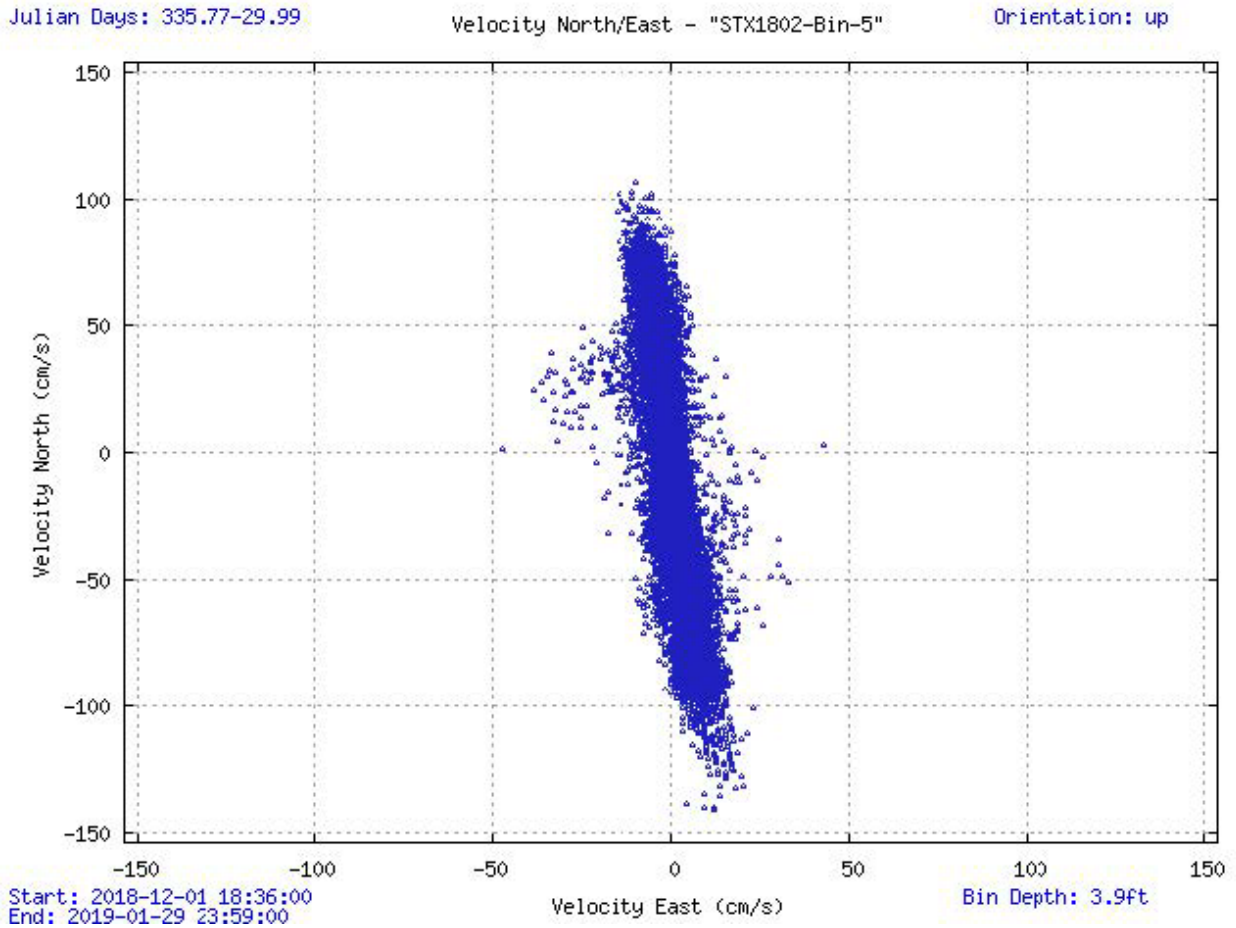


Figure 5-7. Scatter plot of north-versus-east velocity for station STX1802 at the prediction bin, bin 5 at 1.2 m below MLLW.

Julian Days: 363.24-2.40

Orientation: up

Analysis: LSQHA

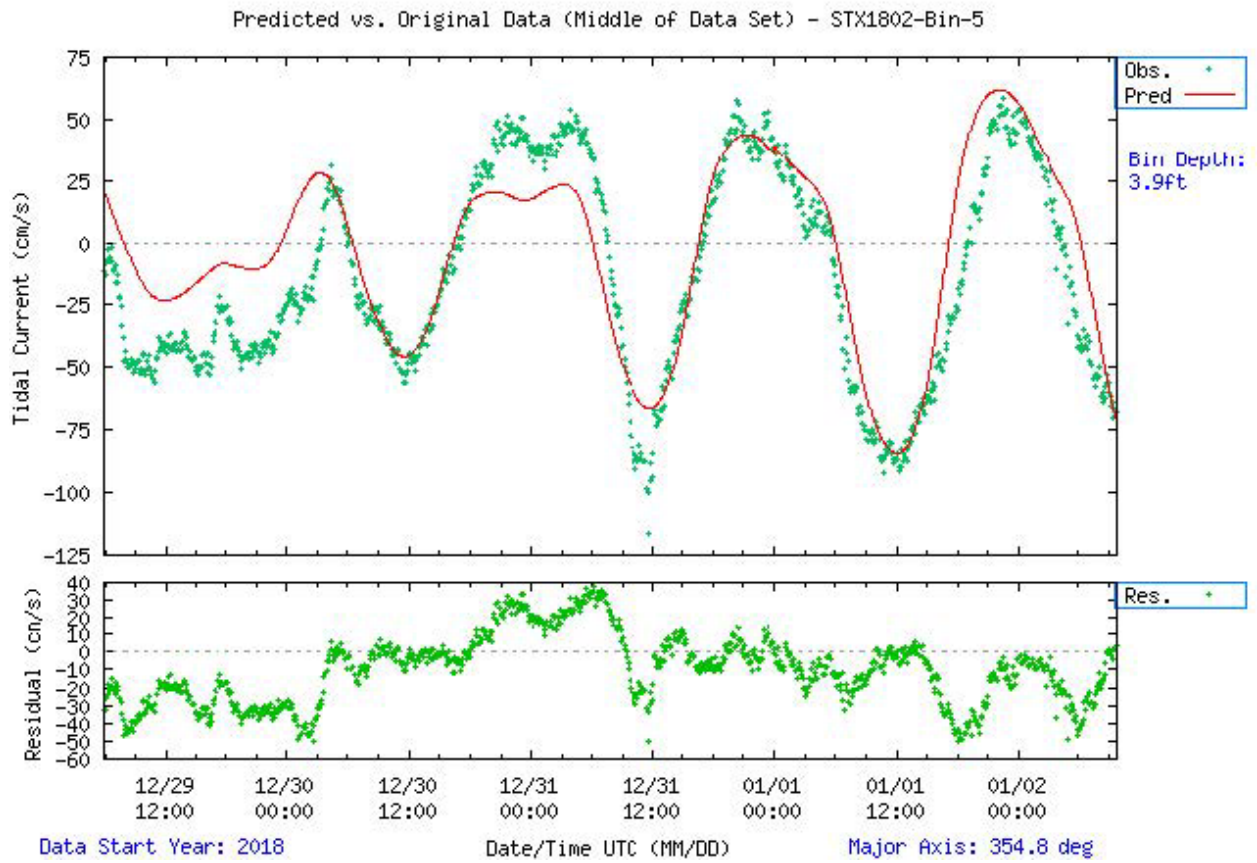


Figure 5-8. Comparison of observed major axis velocity data (green points) to predicted tidal velocity along the major axis for station STX1802. The lower figure shows the non-tidal residual, which is the difference between the predicted and observed velocity from the upper prediction bin.

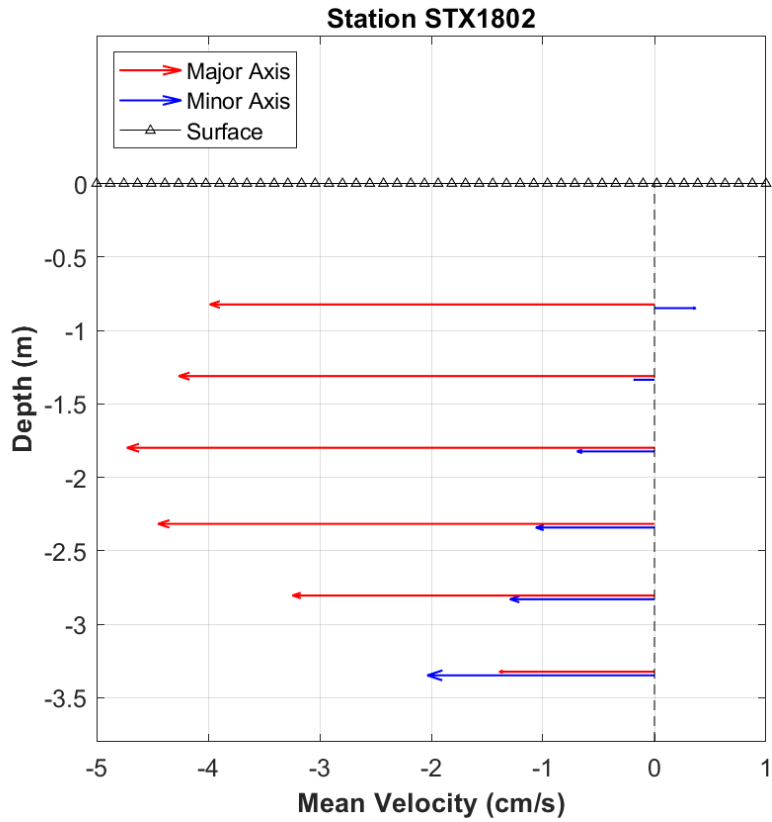


Figure 5-9. STX1802 mean velocity profile by depth. Only depths that passed quality control criteria are shown. This station was configured to collect 0.5-m bins.

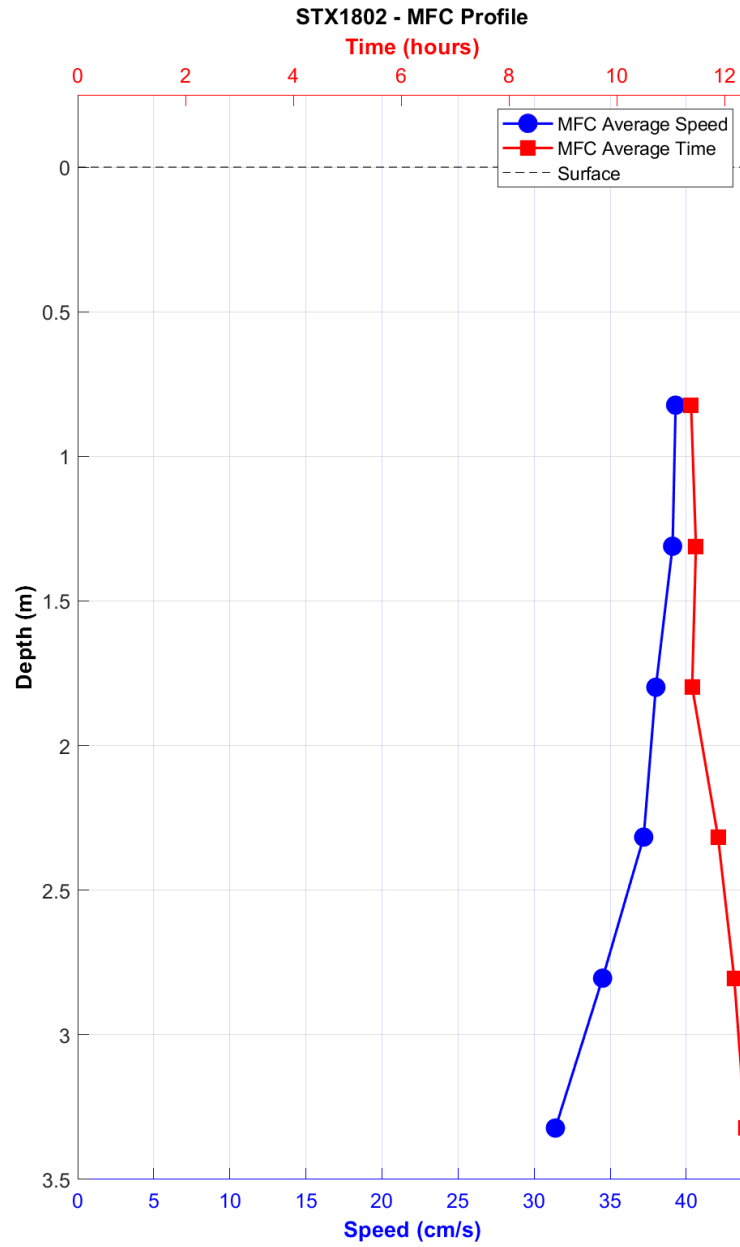


Figure 5-10. STX1802 MFC timing (GI - in red squares) and speed (blue circles) by depth bin.

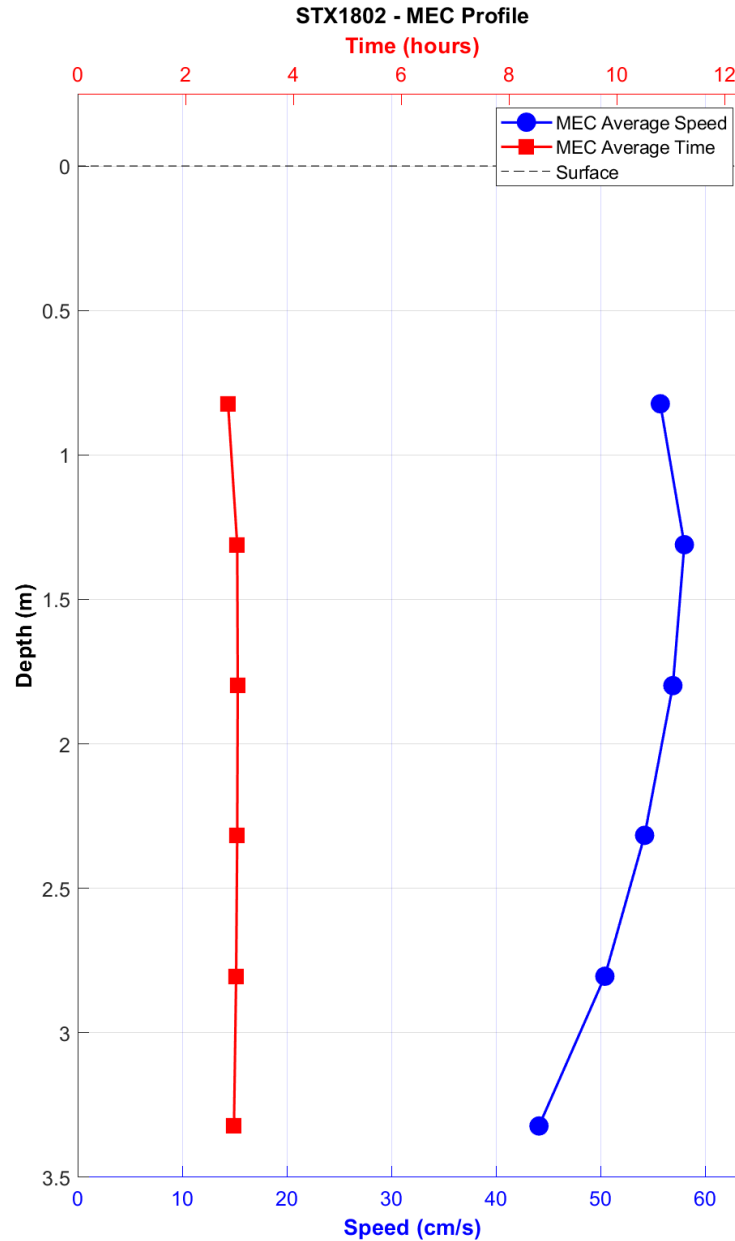


Figure 5-11. STX1802 MEC timing (GI - in red squares) and speed (blue circles) by depth bin.

5.3. STX1813 – Intracoastal Waterway Light 69

This station was deployed for 51 days (December 01, 2017-January 21, 2018) in 3.5 m (11.5 ft) of water. A 2 MHz Nortek (AqD) with a 90° head mounted onto a fiberglass grate collected 20 half-meter bins, 3 of which met quality control criteria for full analysis. Bin 3 is available as a station on TCP, representing an approximate depth of 1.2 m (3.8 ft) below MLLW.

This station is in the southern portion of Laguna Madre, adjacent to the Gulf Intracoastal Waterway, approximately 1.7 nmi northwest of the Queen Isabella Causeway. Observed currents are rectilinear (Figure 5-12), with major axis variance between 97.8 and 98.9%. This station is significantly tidal, which is indicated by the total accounted energy as seen in Figure 5-13. A small mean northwest (flood) current is seen throughout the water column, with maximum speeds at the

surface (Figure 5-14). LSQHA resolved 24 constituents and accounted for 82-83% of the total energy in the velocity data. Mean MFC and MEC speeds range from 38.6-24.7 cm/s (0.8-0.5 kn), and their timing does not vary much with depth (Figures 5-15 and 5-16). The Defant ratio in the upper good bin was 2.75, indicating that this station is mixed, mainly diurnal.

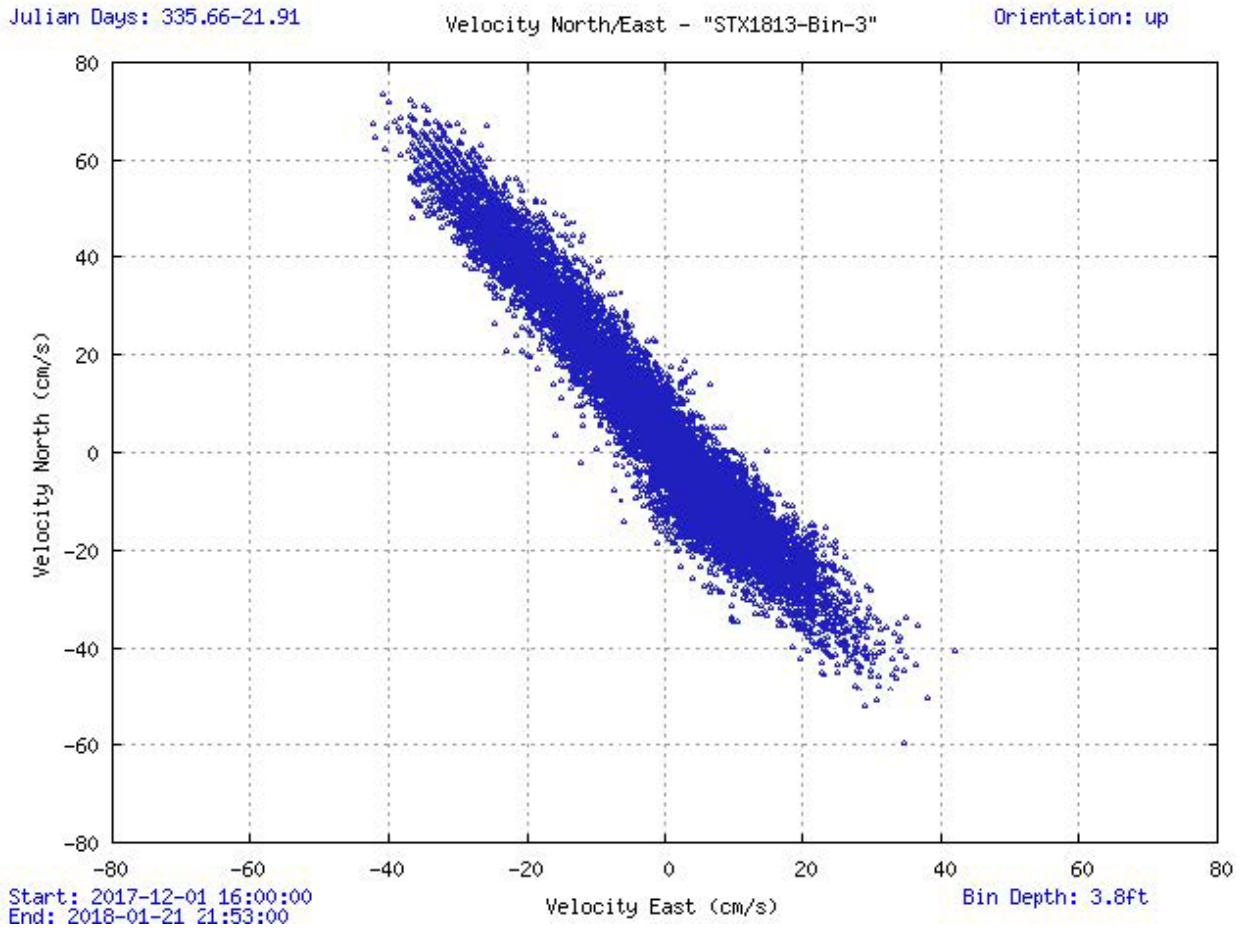


Figure 5-12. Scatter plot of north-versus-east velocity for station STX1813 at the near-surface bin, bin 3 at 1.2 m below MLLW.

Julian Days: 353.20-362.36

Orientation: up

Analysis: LSQHA

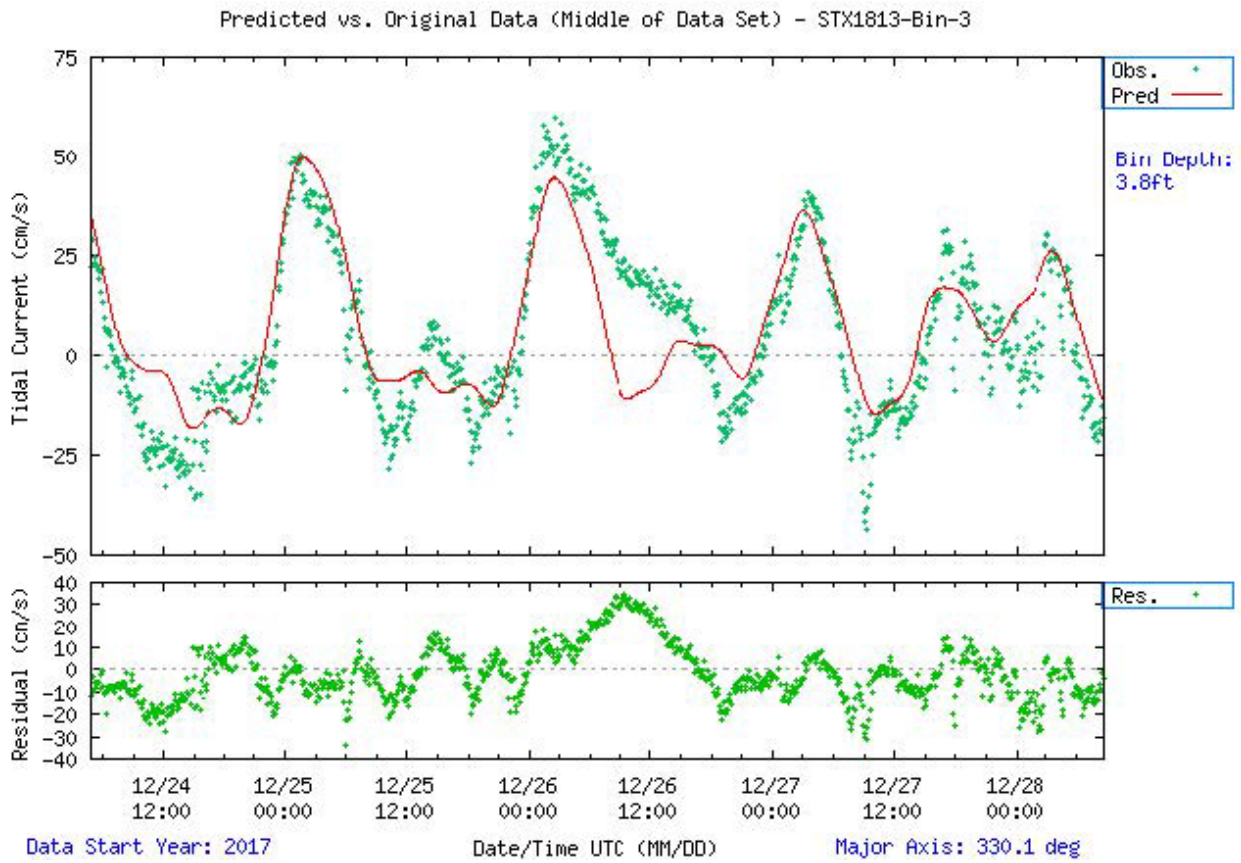


Figure 5-13. Comparison of observed major axis velocity data (green points) to predicted tidal velocity along the major axis for station STX1813. The lower figure shows the non-tidal residual, which is the difference between the predicted and observed velocity from the upper panel.

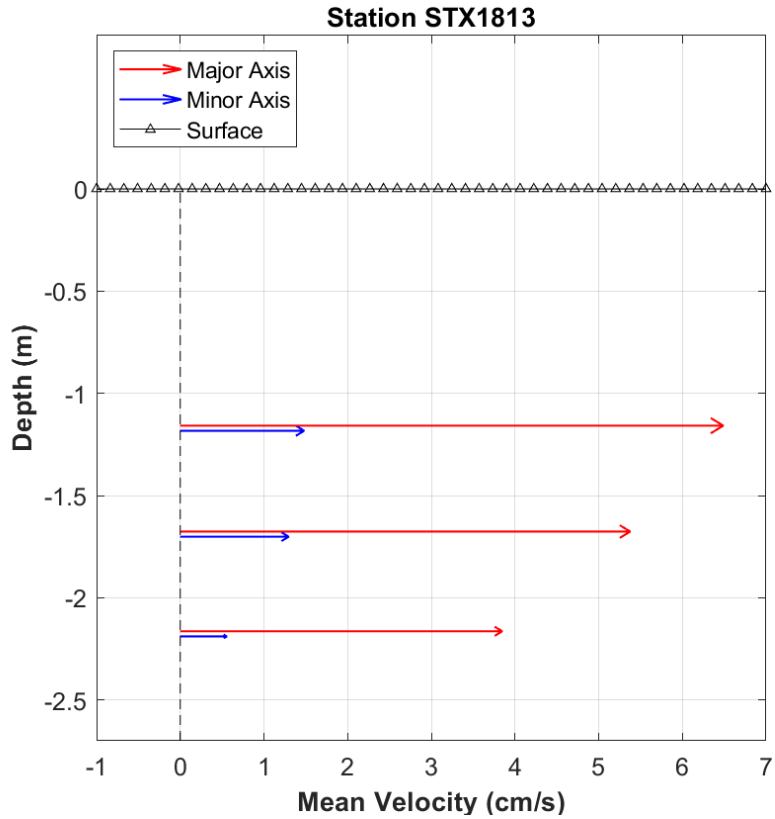


Figure 5-14. STX1813 mean velocity profile by depth. Only depths that passed quality control criteria are shown. This station was configured to collect 0.5-m bins.

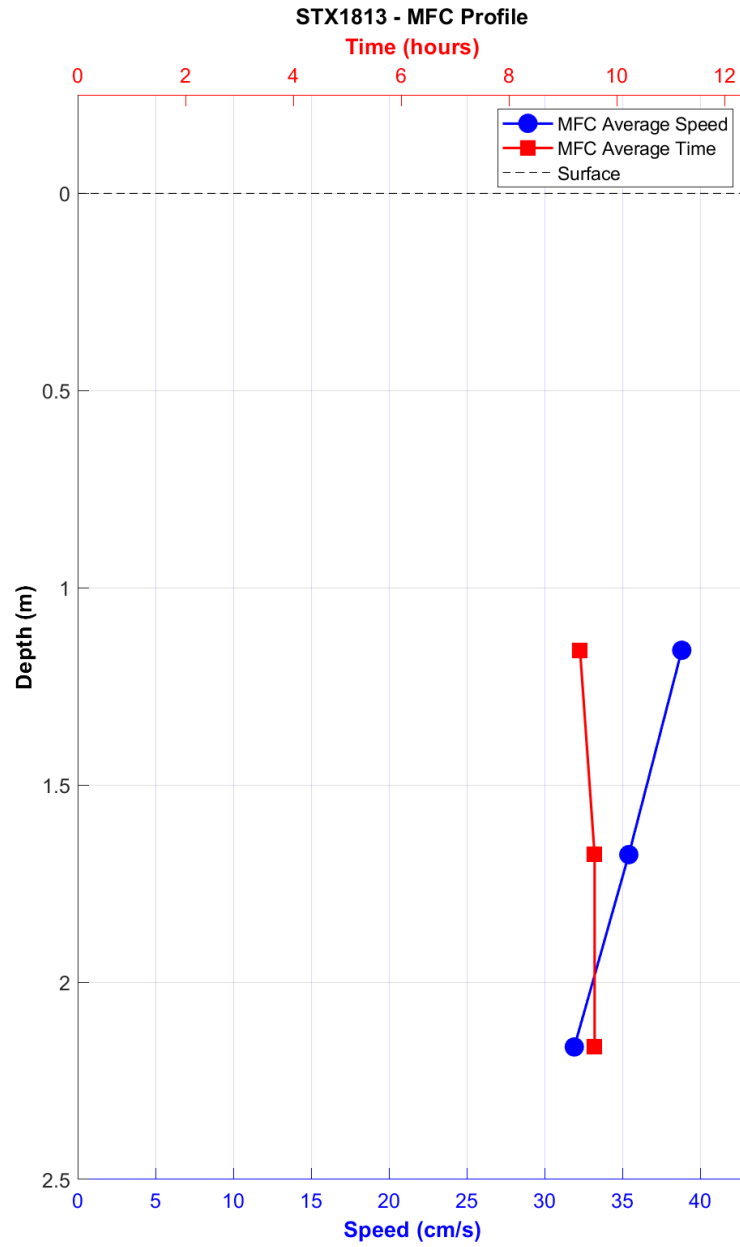


Figure 5-15. STX1813 MFC timing (GI - in red squares) and speed (blue circles) by depth bin.

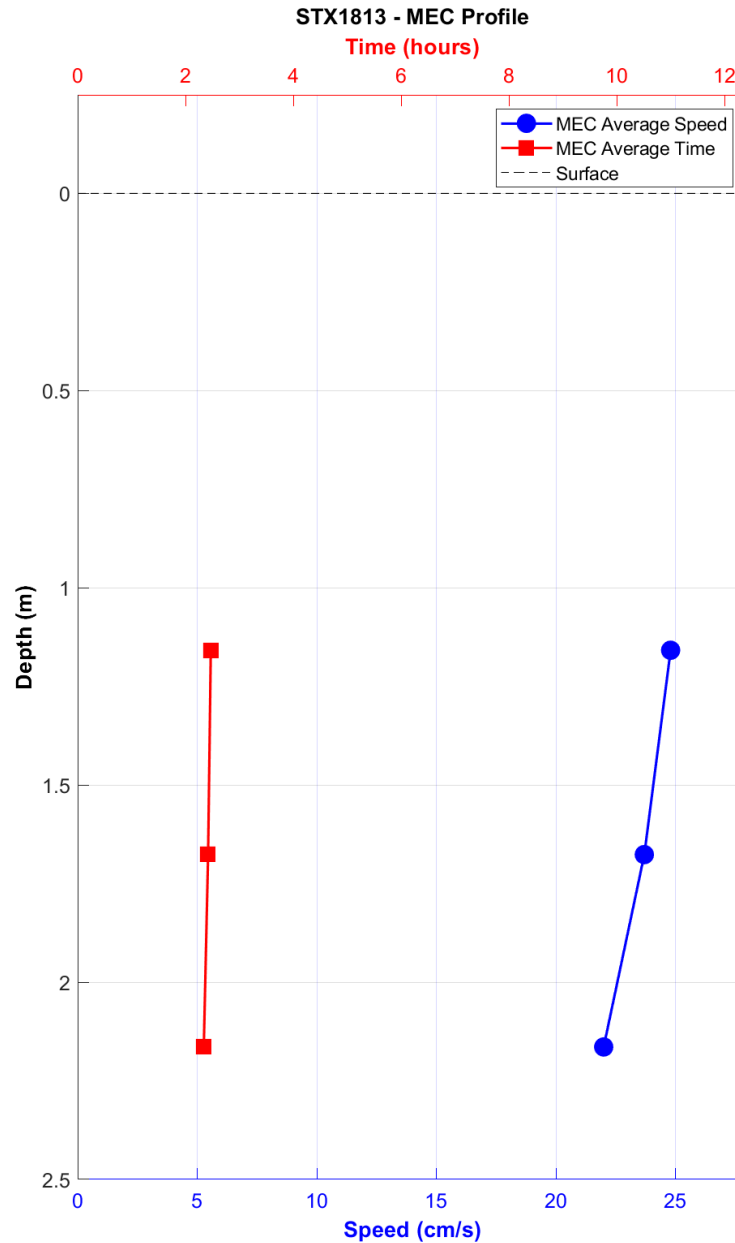


Figure 5-16. STX1813 MEC timing (GI - in red squares) and speed (blue circles) by depth bin.

5.4. STX1814 – Queen Isabella Causeway Bridge

This station was deployed for 184 days (May 05, 2018–November 05, 2018) in 5.5 m (18.0 ft) of water. A 600 kHz Nortek ADCP configured for horizontal measurements was mounted at a depth of 3.0 m (9.8 ft) on bridge cribbing using a clamp and pole as described in section 3.4. Twenty 2.0-m bins were collected, 16 of which met quality control criteria for full analysis. Bin 14 is available on TCP representing 28.5 m (93.5 ft) from the sensor, in about the center of the channel.

Queen Isabella Causeway Bridge crosses the southern end of the Laguna Madre between Port Isabel and South Padre Island. This station was mounted south of the road deck and oriented toward the west to look across the channel of the Gulf Intracoastal Waterway where it passes under the bridge. Observed currents are very rectilinear, with major axis variance of 94-99% throughout all good bins

(Figure 5-17). This station is significantly tidal, as seen in Figure 5-18. LSQHA resolved 32 constituents and accounted for 87-92% of the total energy in the velocity data. A small mean southeasterly (ebb) current was observed, strongest near the sensor and becoming almost negligible near the center of the channel (Figure 5-19). MFC and MEC speeds both peaked at 43.2 cm/s (0.8 kn), and their timing does not vary much with distance (Figures 5-20 and 5-21). The Defant ratio in the outer good bin was 2.66, indicating that this station is mixed, mainly diurnal.

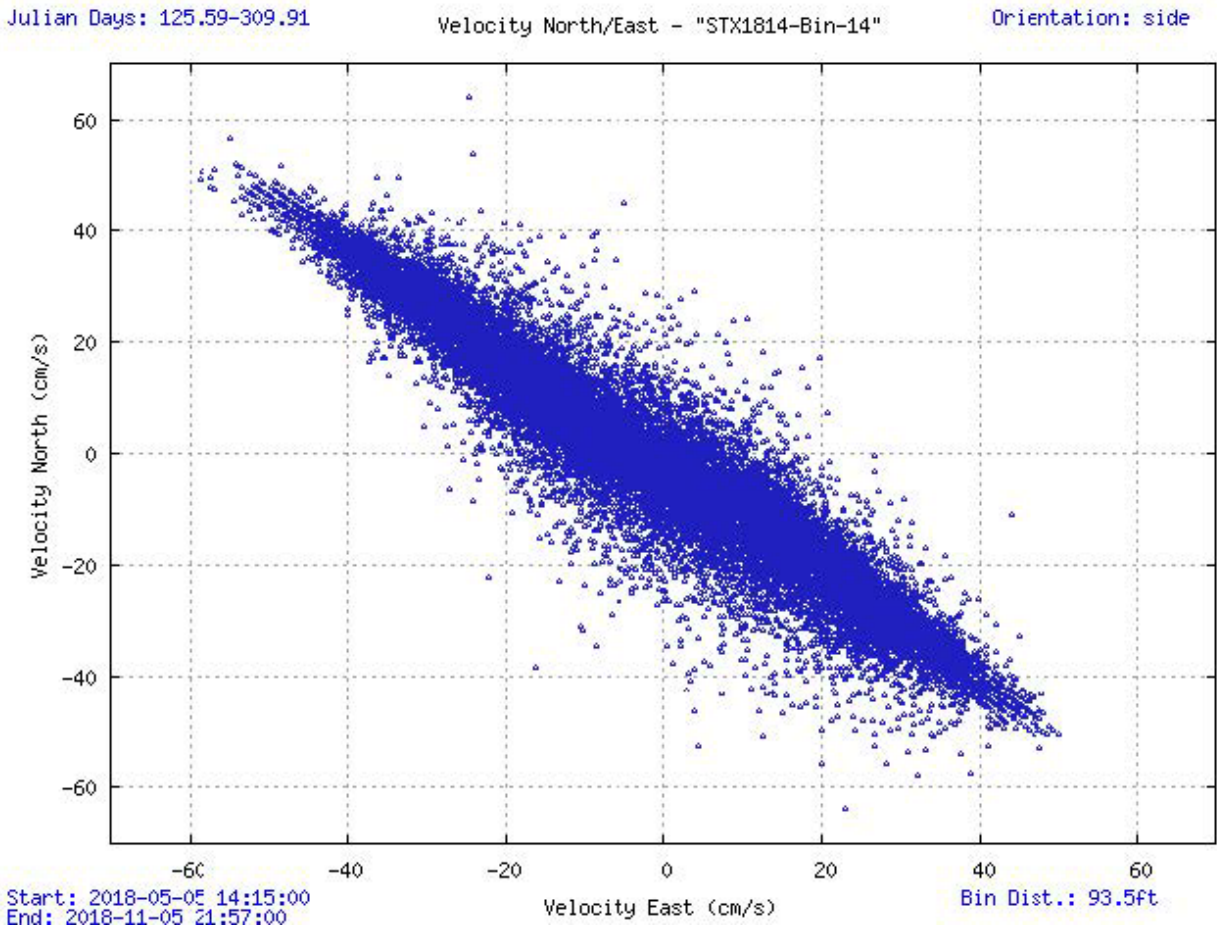


Figure 5-17. Scatter plot of north-versus-east velocity for station STX1814 at the center of the channel, 28.5 m from the sensor.

Julian Days: 213.13-221.47

Orientation: side

Analysis: LSQHA

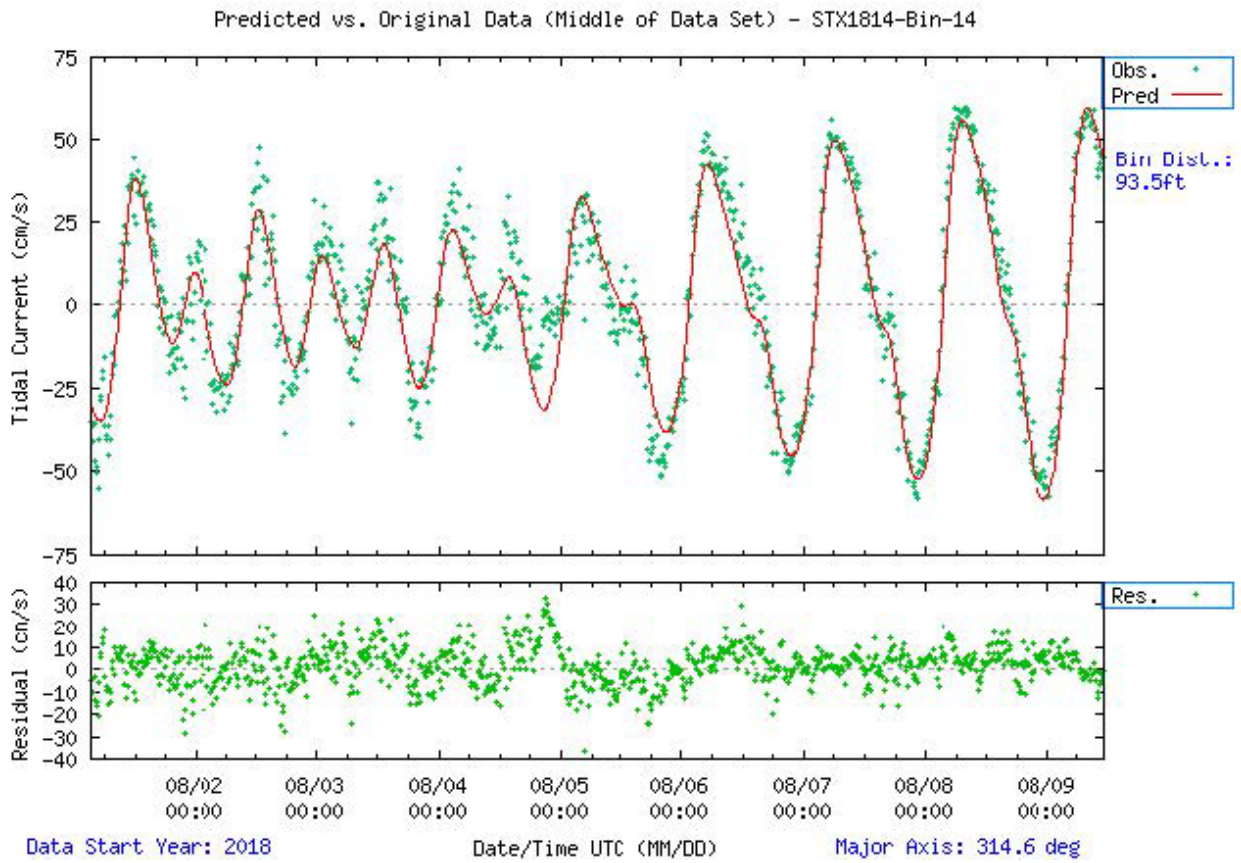


Figure 5-18. Comparison of observed major axis velocity data (green points) to predicted tidal velocity along the major axis for station STX1814. The lower figure shows the non-tidal residual, which is the difference between the predicted and observed velocity from the upper panel.

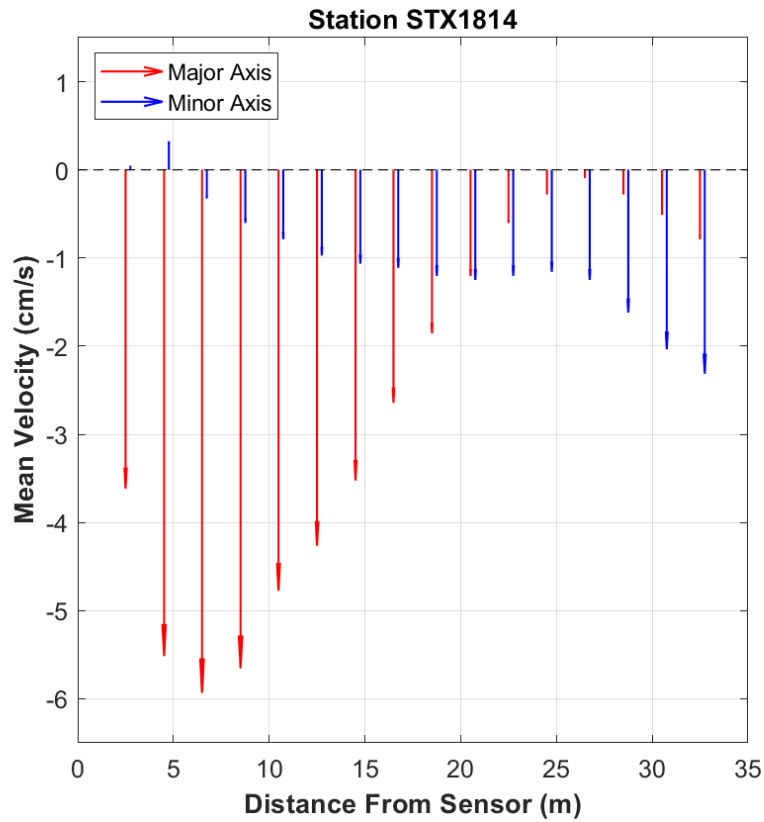


Figure 5-19. STX1814 mean velocity profile by distance bin. Only distances that passed quality control criteria are shown. This station was configured to collect 2.0-m bins.

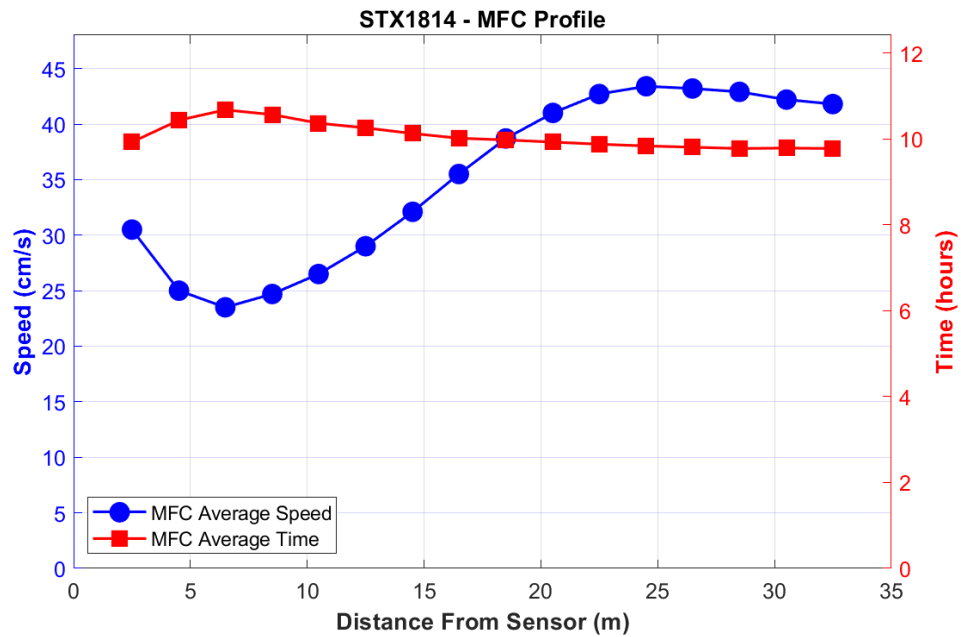


Figure 5-20. STX1814 MFC timing (GI - in red squares) and speed (blue circles) by distance bin.

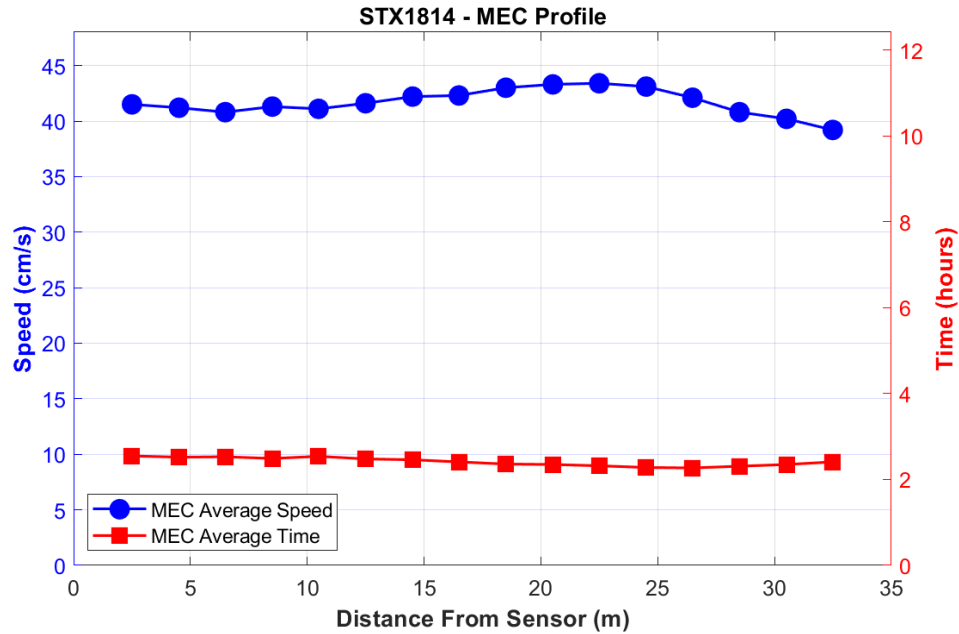


Figure 5-21. STX1814 MEC timing (GI - in red squares) and speed (blue circles) by distance bin.

5.5. STX1820 – Brazos Santiago Pass Entrance

This station was deployed for 54 days (December 9, 2017-January 31, 2018) in 12.3 m (40.4 ft) of water. A TRDI Workhorse 600 kHz ADCP mounted in an H-TRBM collected 23 1-m bins of data, 9 of which met quality control criteria for full analysis. Bins 1, 6, and 9 are published in the TCPs, representing approximate depths of 9.8 m, 4.8 m, and 1.8 m (32.2 ft, 15.7 ft, and 5.9 ft) below MLLW, respectively.

Brazos Santiago Pass separates South Padre Island from Brazos Island and is the seaward entrance for vessels transiting to the ports of Brownsville and Port Isabel. This station is the most seaward of 2 locations occupied within the pass for this survey and is located to the south of the shipping channel. Observed currents are extremely rectilinear, with major axis variance of 99.1-99.5% (Figure 5-22). This station is tidal, which is indicated by the total accounted energy, as seen in Figure 5-23. A mean westerly (flood) current is seen throughout the water column (Figure 5-24). LSQHA resolved 24 constituents and accounted for 83-87% of the total energy in the velocity data. Mean MFC and MEC speeds have a range of 71-79 cm/s (1.4-1.6 kn), and their timing does not vary much with depth (Figures 5-25 and 5-26). The Defant ratio in the upper good bin was 3.68, indicating that this station is diurnal.

Julian Days: 343.00-31.83

Velocity North/East - "STX1820-Bin-9"

Orientation: up

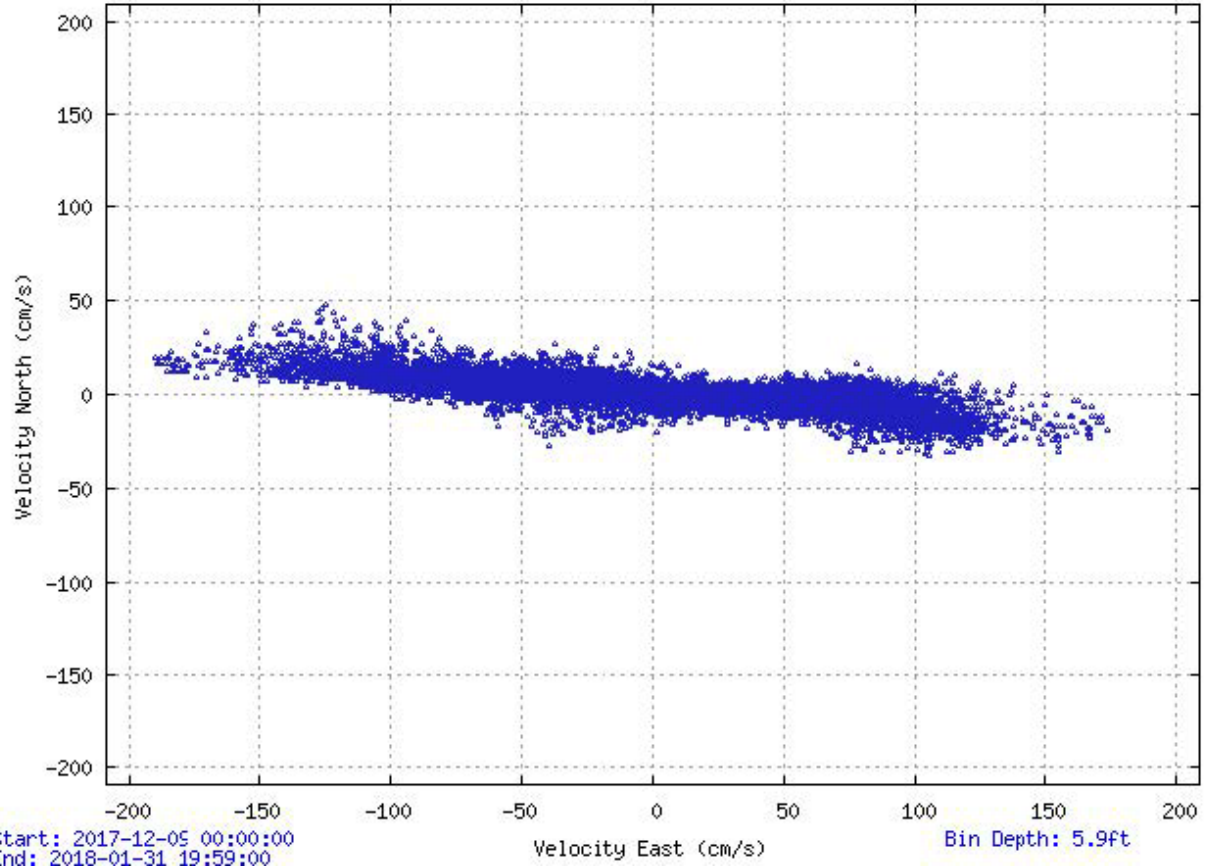


Figure 5-22. Scatter plot of north-versus-east velocity for station STX1820 at the near-surface bin, bin 9 at 1.8 m below MLLW.

Julian Days: 2.33-6.99

Orientation: up

Analysis: LSQHA

Predicted vs. Original Data (Middle of Data Set) - STX1820-Bin-9

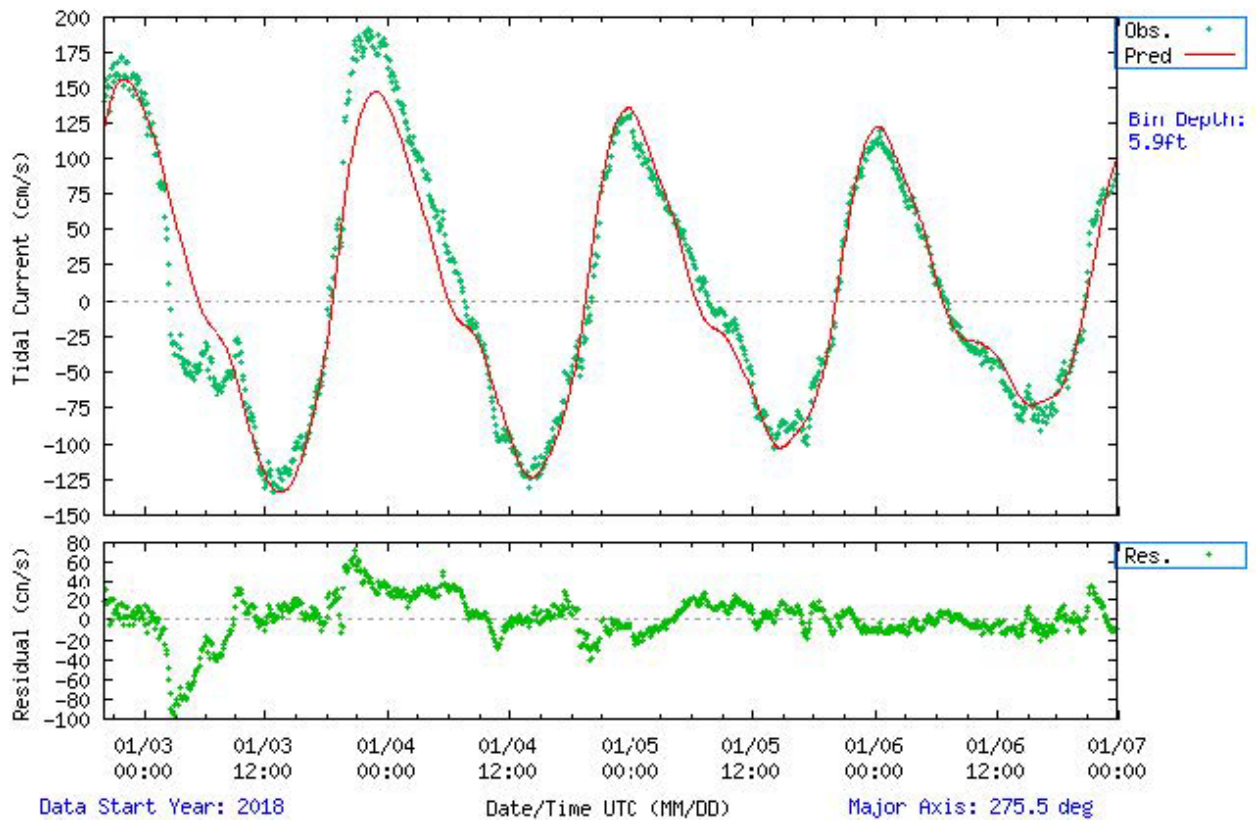


Figure 5-23. Comparison of observed major axis velocity data (green points) to predicted tidal velocity along the major axis for station STX1820. The lower figure shows the non-tidal residual, which is the difference between the predicted and observed velocity from the upper panel.

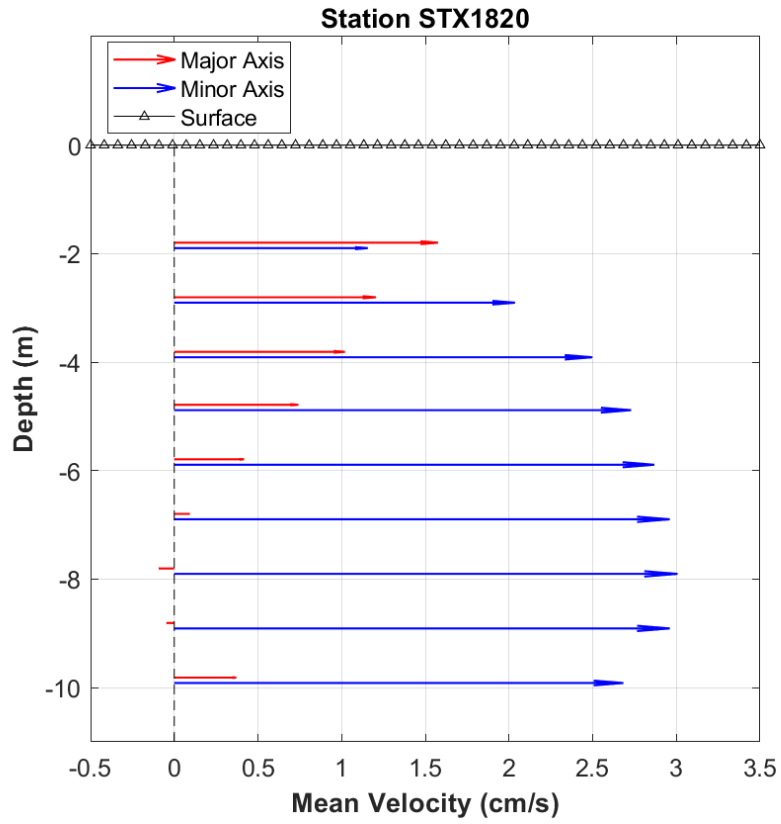


Figure 5-24. STX1820 mean velocity profile by depth. Only depths that passed quality control criteria are shown. This station was configured to collect 1.0-m bins.

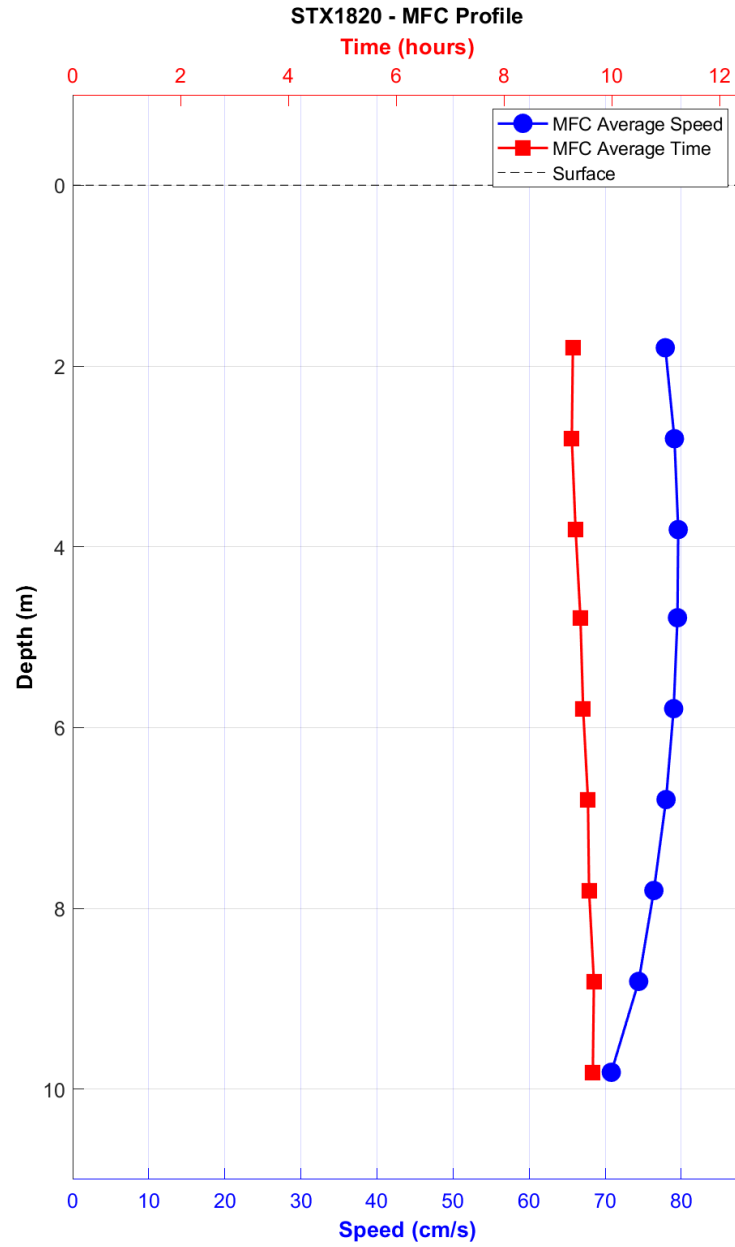


Figure 5-25. STX1820 MFC timing (GI – red squares) and speed (blue circles) by depth bin.

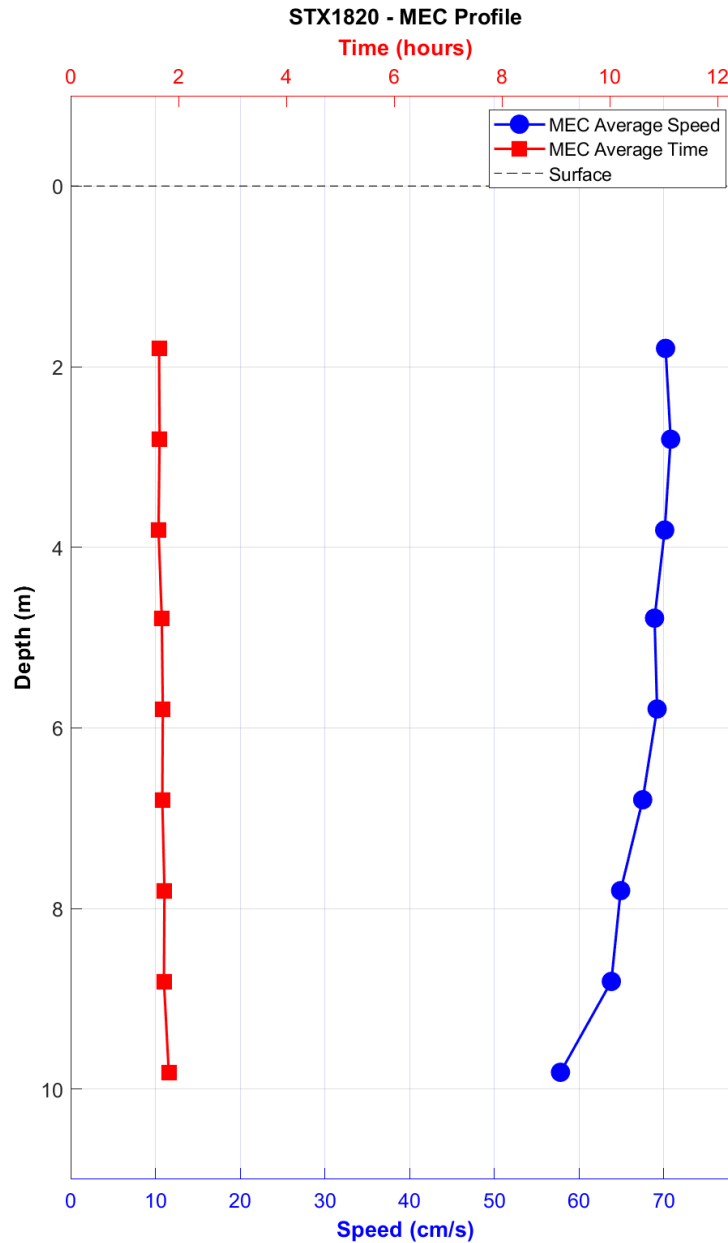


Figure 5-26. STX1820 MEC timing (GI – red squares) and speed (blue circles) by depth bin.

5.6. STX1821 – Brazos Santiago Pass (SPIP)

This station Brazos Santiago Pass (SPIP) was deployed for 185 days (August 03, 2018-February 04, 2019) in 5 m (16.4 ft) of water. A Nortek AWAC 400 kHz ADCP mounted on a sled attached to an I-beam collected 30 4-m bins of data, all of which met quality control criteria for full analysis. Bin 29 is published in the TCPs, representing an approximate distance of 117.0 m (383.9 ft) from the instrument.

The SPIP is on the north side of the shipping channel at about the midpoint of the pass. Observed currents are extremely rectilinear, with major axis variance of 97.0-99.4% (Figure 5-27). This station is moderately tidal, which is indicated by the total accounted energy as seen in Figure 5-28. A mean westerly (flood) current is seen throughout the water column (Figure 5-29). LSQHA

resolved 24 constituents and accounted for 58-84% of the total energy in the velocity data. Mean MFC and MEC speeds have a range of 51-56 cm/s (1.0-1.1 kn), and their timing does not vary much with depth (Figures 5-30 and 5-31). The Defant ratio in the outer good bin was 2.54, indicating that this station is mixed, mainly diurnal.

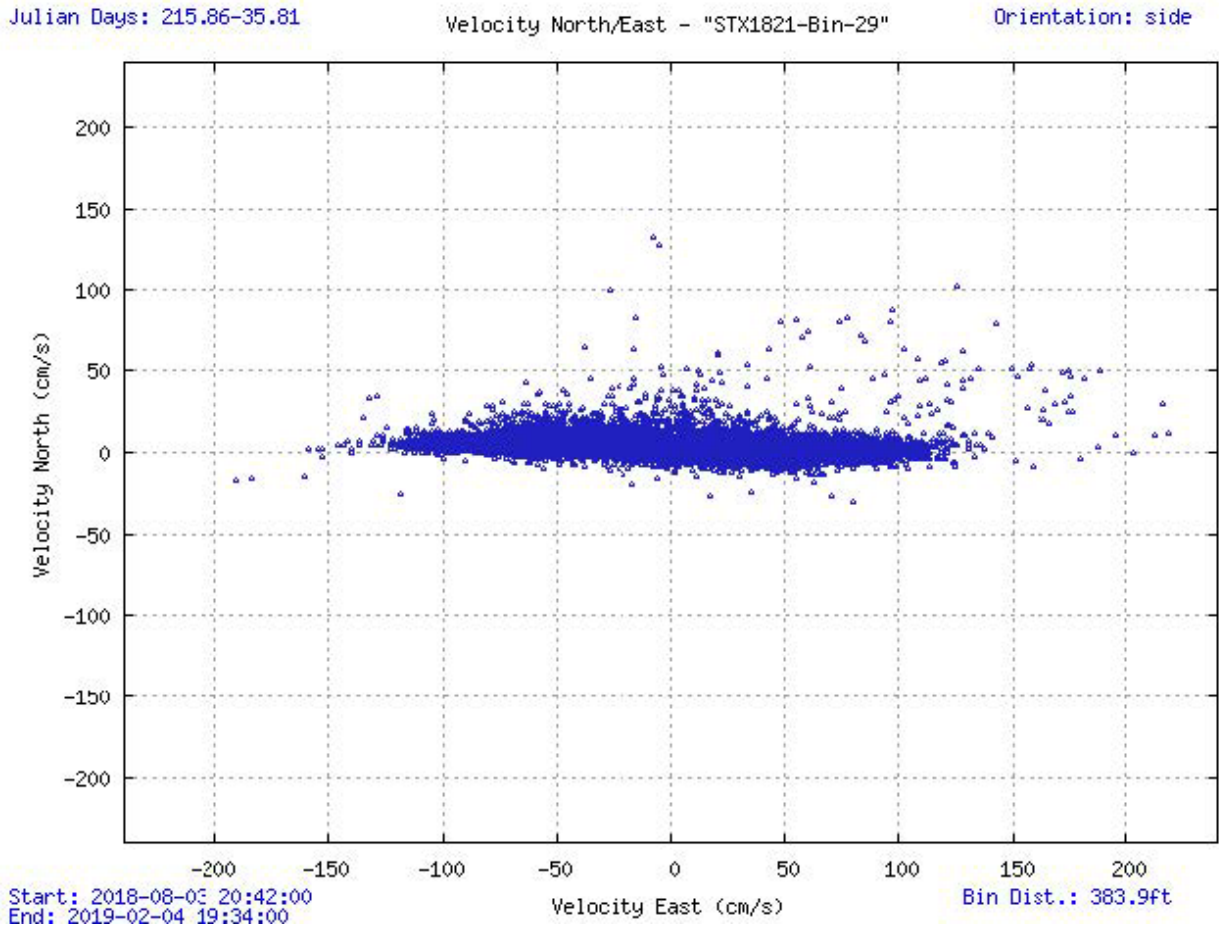


Figure 5-27. Scatter plot of north-versus-east velocity for station STX1821 at bin 29 (the prediction bin).

Julian Days: 305.85-310.01

Orientation: side

Analysis: LSQHA

Predicted vs. Original Data (Middle of Data Set) - STX1821-Bin-29

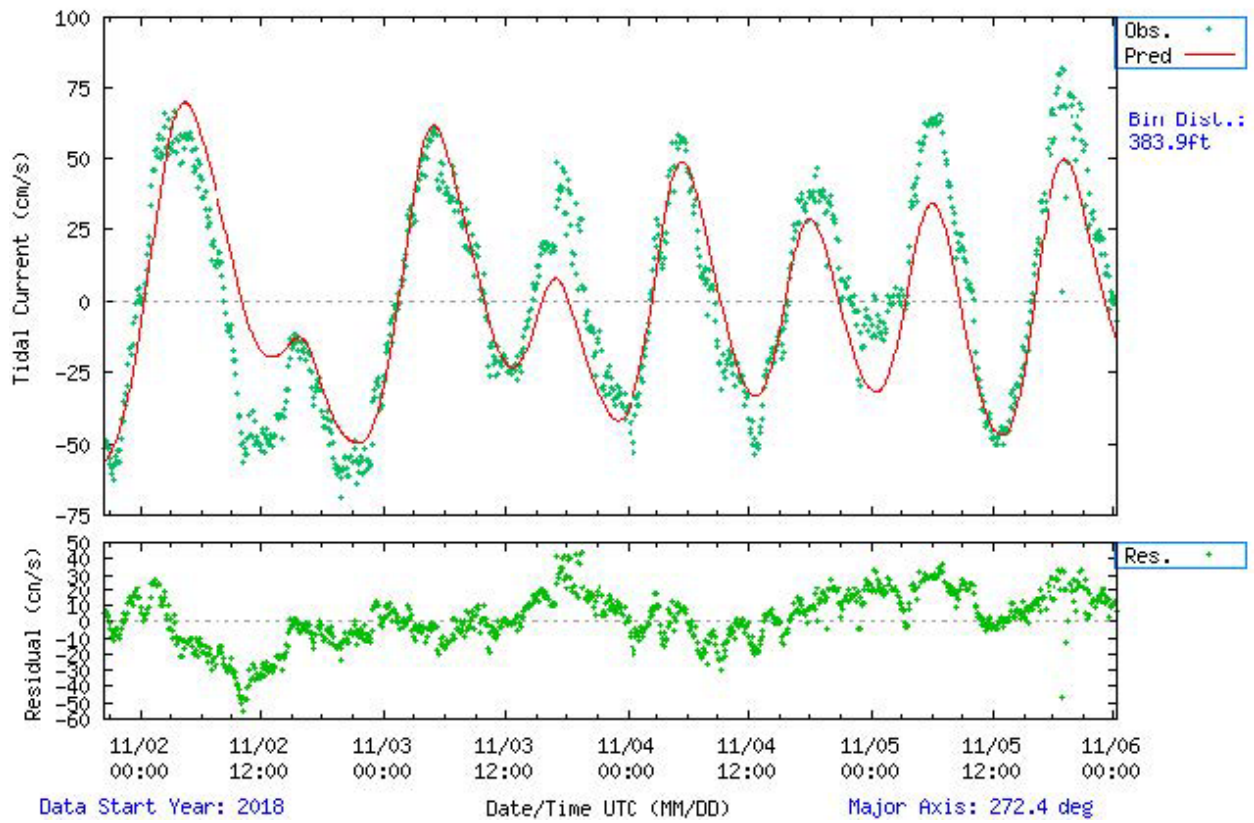


Figure 5-28. Comparison of observed major axis velocity data (green points) to predicted tidal velocity along the major axis for station STX1821. The lower figure shows the non-tidal residual, which is the difference between the predicted and observed velocity from the upper panel.

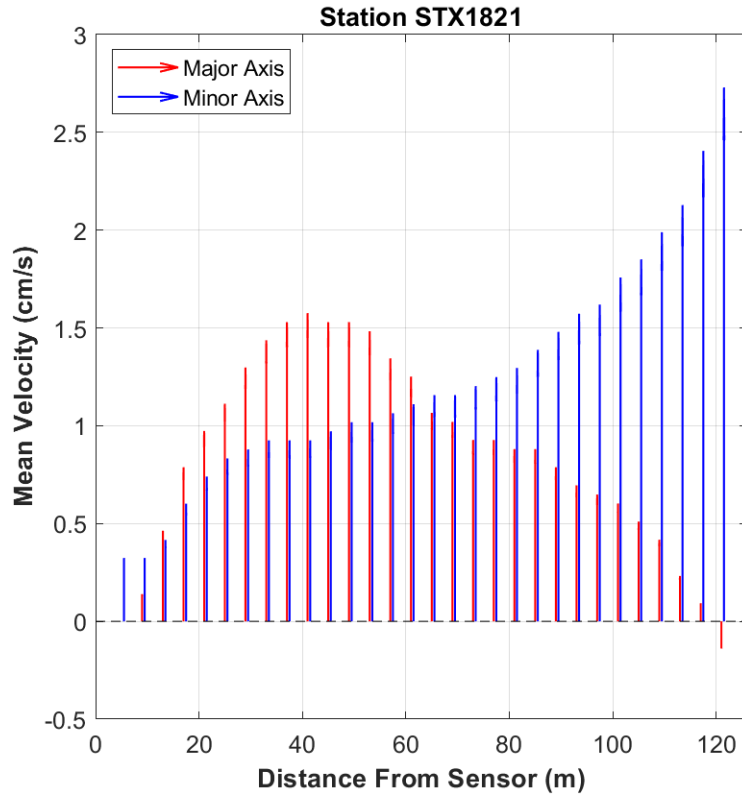


Figure 5-29. STX1821 mean velocity profile by distance. This station was configured to collect 4.0-m bins.

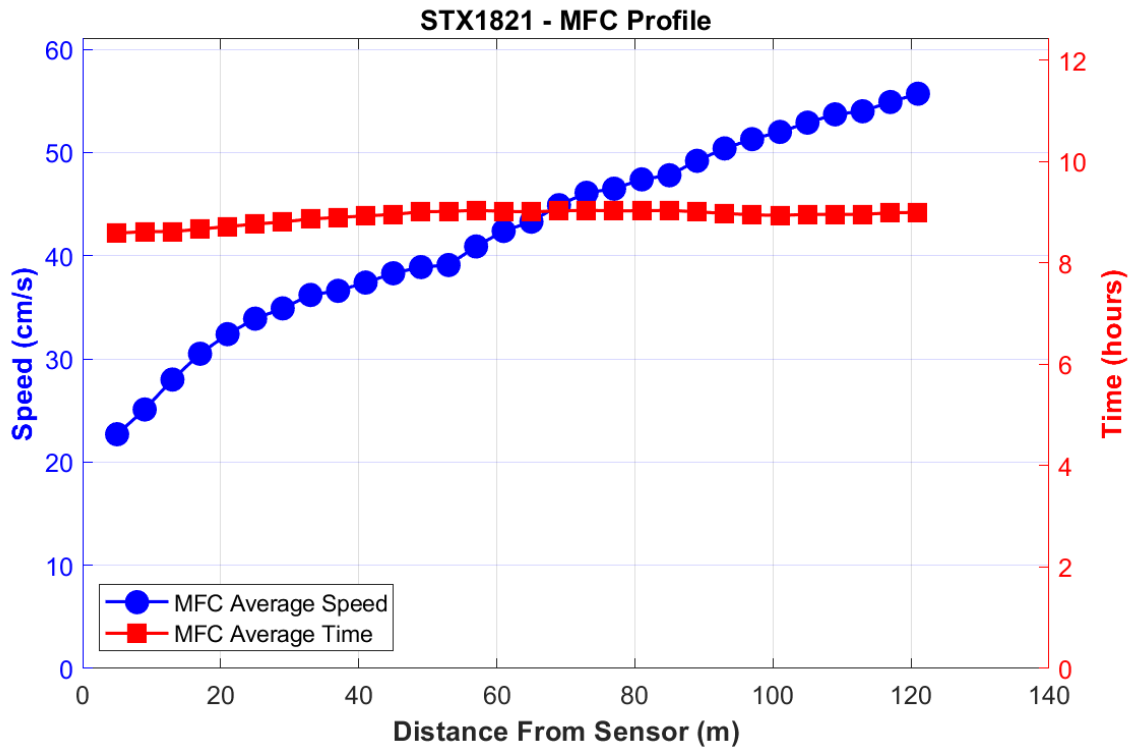


Figure 5-30. STX1821 MFC timing (GI - in red squares) and speed (blue circles) by depth bin.

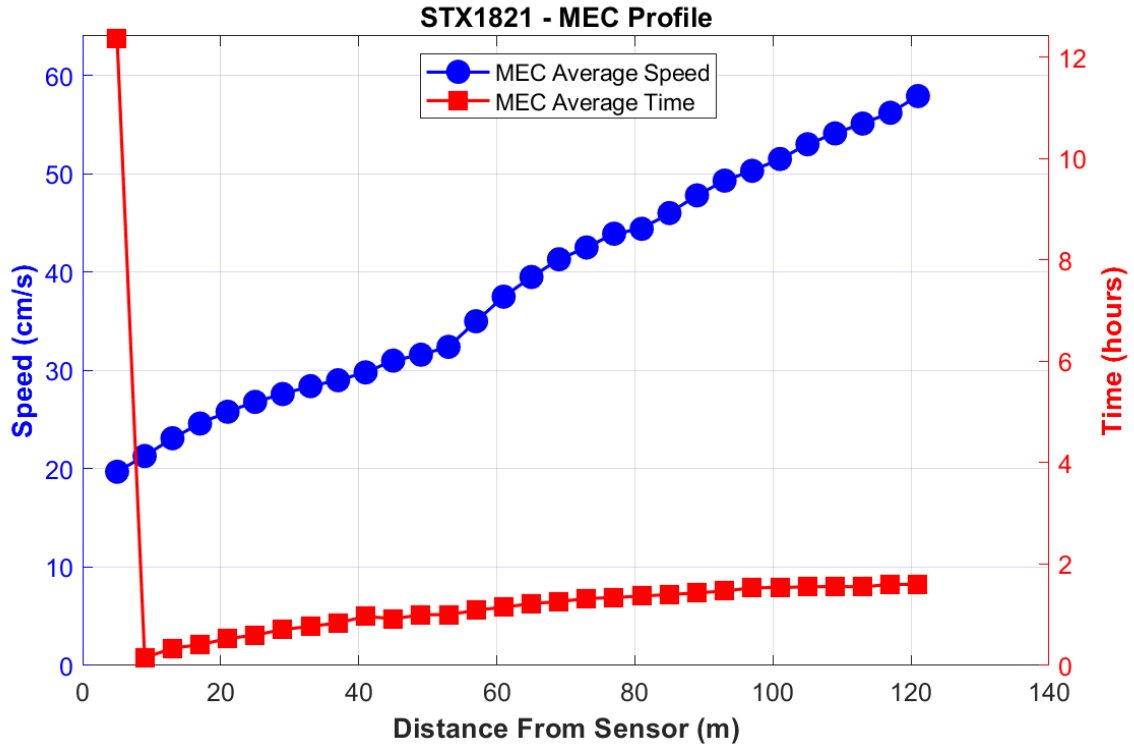


Figure 5-31. STX1821 MEC timing (GI - in red squares) and speed (blue circles) by distance bin. The change in GI timing from bin 1 to bin 2 is due to crossing the maximum GI threshold of 12.42 hours. The GI time for bin 1 is 12.37, and 0.15 for bin 2.

5.7. STX1822 – Port Isabel Channel, North End

This station was deployed for 37 days (May 04, 2018-June 11) in 8.6 m (28.2 ft) of water. A 600 kHz Nortek AqD ADCP configured for horizontal measurements was mounted at a depth of 5.0 m (16.4 ft) on a pier structure using a clamp and pole as described in section 3.4. Twenty 2.0-m bins were collected, 18 of which met quality control criteria for full analysis. Bin 13 is available on TCP representing 26.5 m (86.9 ft) from the sensor, on the western edge of the channel.

Port Isabel Channel is the southern section of the waterway that joins the lower Laguna Madre with the Brownsville shipping channel between Long Island and Port Isabel. Observed currents are rectilinear, with major axis variance of 90-97% throughout all good bins (Figure 5-31). This station is moderately tidal, as seen in Figure 5-32. LSQHA resolved 24 constituents and accounted for 63-81% of the total energy in the velocity data. A small mean southerly (ebb) current was observed, strongest near the sensor and becoming almost negligible near the center of the channel. (Figure 5-33). Mean MFC and MEC speeds have a range of 18-22 cm/s (0.360.44 kn), and their timing does not vary much with distance (Figures 5-34 and 5-35). The Defant ratio in the outer good bin is 2.38, indicating that this station is mixed, mainly diurnal.

Julian Days: 124.90-162.80

Velocity North/East - "STX1822-Bin-13"

Orientation: side

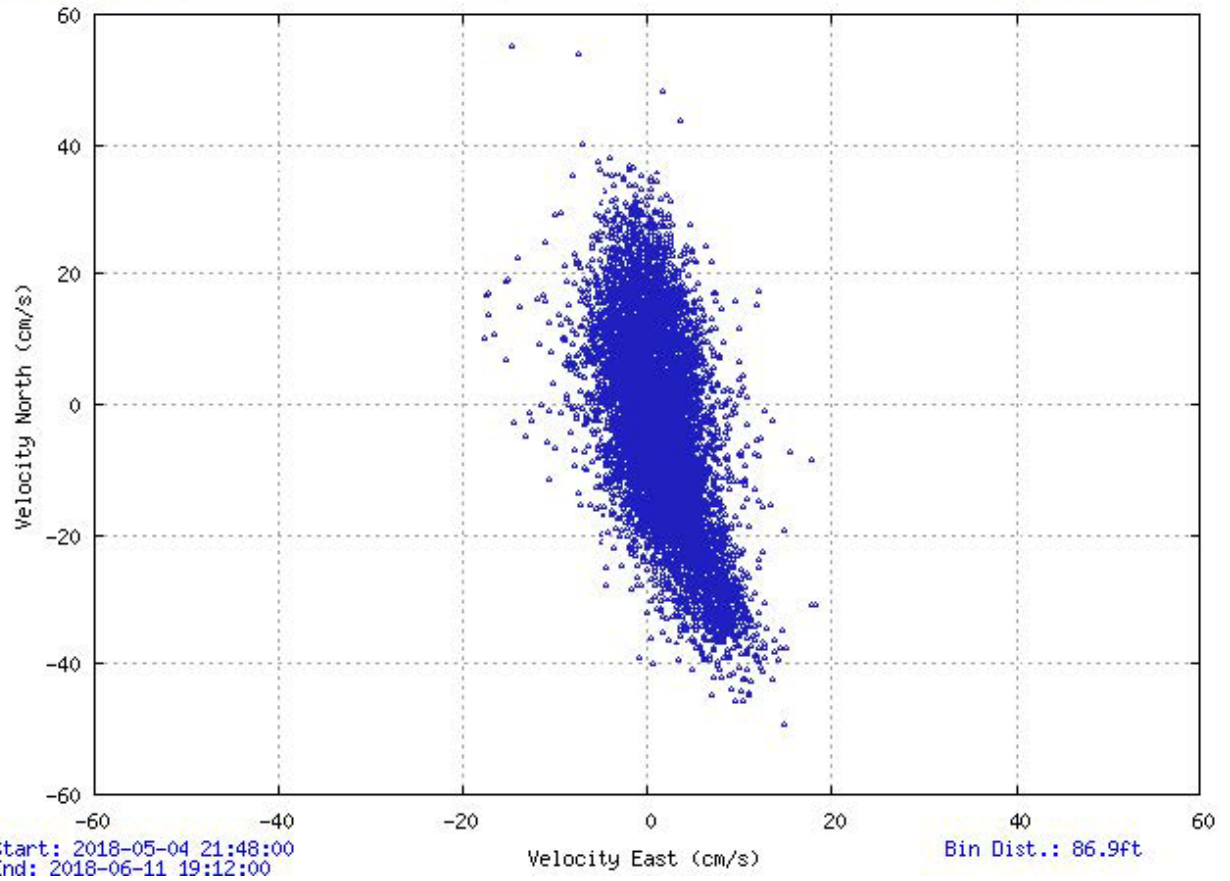


Figure 5-32. Scatter plot of north-versus-east velocity for station STX1822 at bin 13 (the prediction bin)

Julian Days: 141.77-145.93

Orientation: side

Analysis: LSQHA

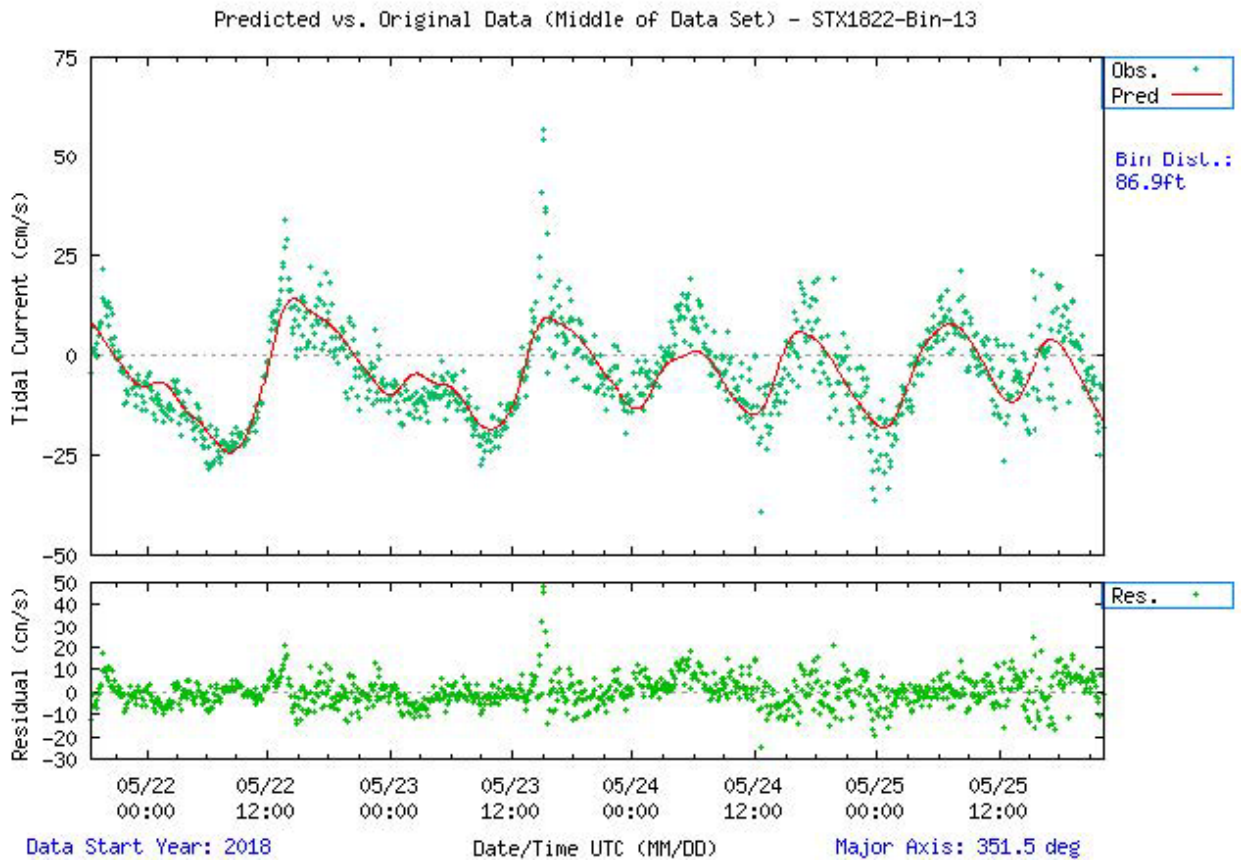


Figure 5-33. Comparison of observed major axis velocity data (green points) to predicted tidal velocity along the major axis for station STX1822. The lower figure shows the non-tidal residual, which is the difference between the predicted and observed velocity from the upper panel.

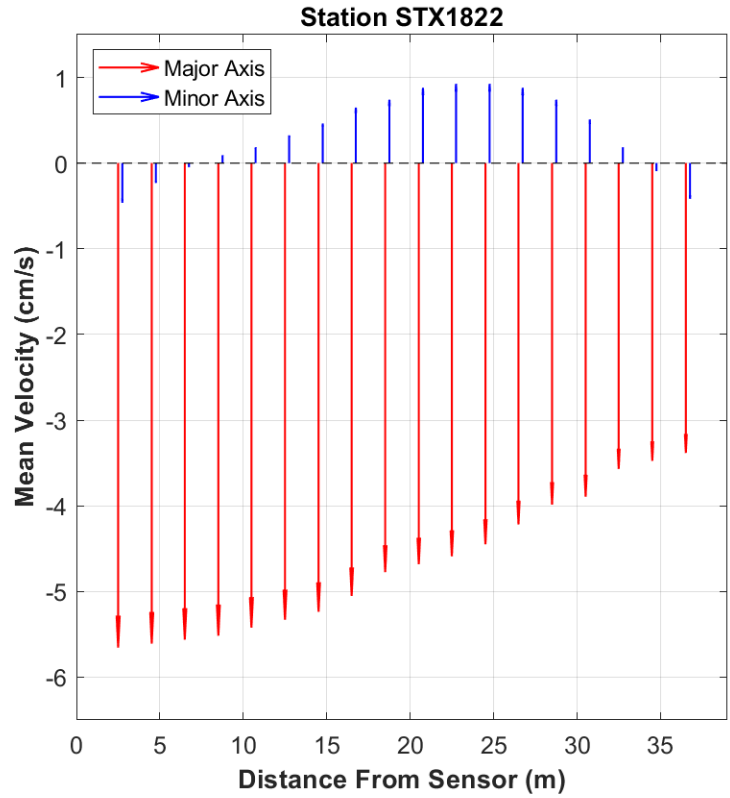


Figure 5-34. STX1822 mean velocity profile by distance. This station was configured to collect 2.0 m bins.

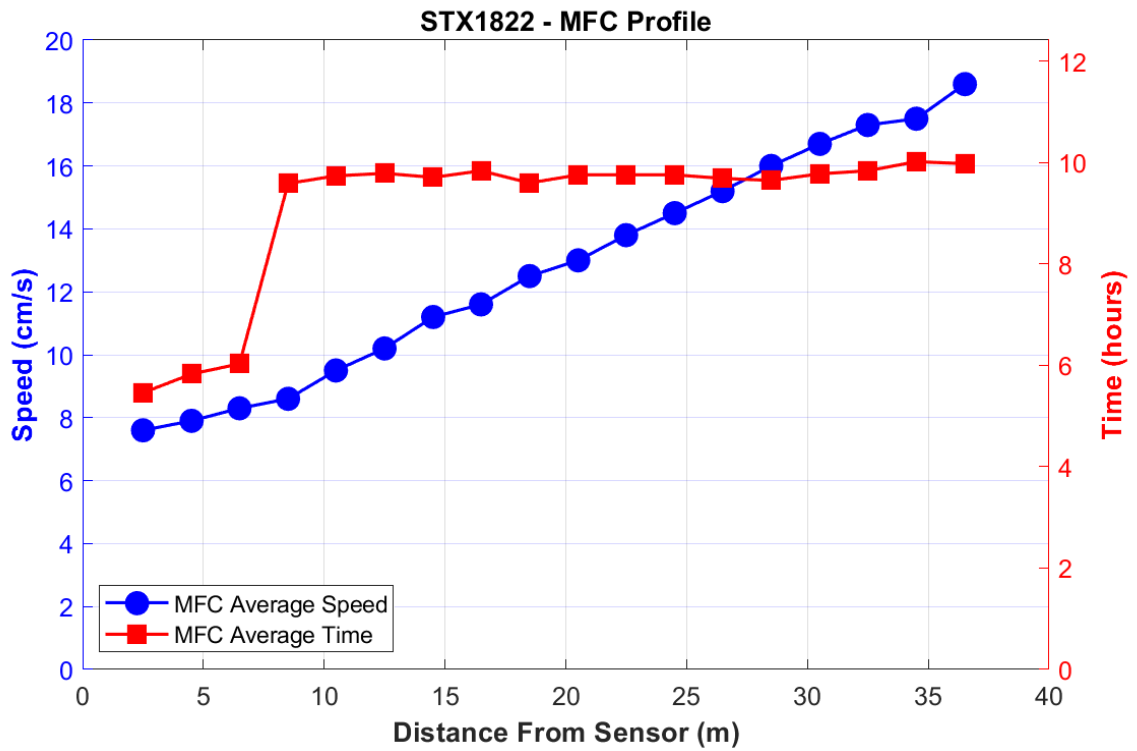


Figure 5-35. STX1822 MFC timing (GI - in red squares) and speed (blue circles) by distance bin.

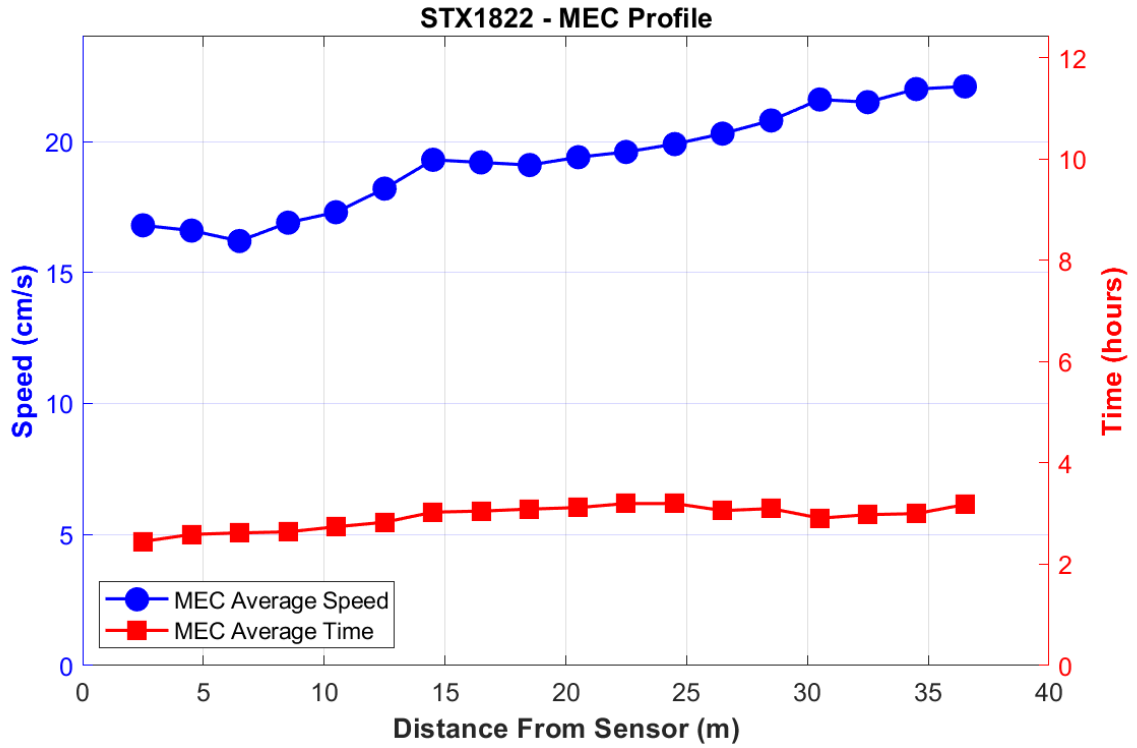


Figure 5-36. STX1822 MEC timing (GI - in red squares) and speed (blue circles) by distance bin.

6. SPATIAL VARIATION

6.1. Harmonic constituents

Harmonic constituents were generated for all stations in this study using the methods described in section 3.6. Analyses of these stations along the Texas coast reveal unique hydrodynamics. Most locations along the U.S. coast exhibit semidiurnal tidal current (and thus tidal water levels) harmonic signal. This is due to the near dominance everywhere of the M_2 tidal constituent (the semidiurnal lunar tide, i.e., the twice daily gravitational pull of the moon on all the world's oceans). As the M_2 is normally the largest constituent followed by S_2 (the semidiurnal solar tide), most coastlines enjoy a twice daily (semi-diurnal) rise and fall of the tide, with the difference in the timing of their periods creating the spring (maximum) and neap (minimal) tidal signal that is reflected in the monthly phases of the Moon, full/new moons, and first/last quarters, respectively.

However, in most of the Gulf of Mexico— especially along the Texas and Mexico coast— the K_1 or O_1 tidal constituents dominate. These two harmonic constituents combine to form the lunar diurnal tide, representing the once-daily tidal bulge maximized when the Moon is at its northernmost or southernmost declination. These tidal forces are at a minimum when the Moon is over the equator. The hydrodynamics (Parker, 2007) resulting from the unique shape of the Gulf of Mexico, and extending to the east end of the Caribbean Sea, reduces the amplitudes of the M_2 tidal constituent. These hydrodynamics create a tidal node (also known as an “amphidromic point”) near the middle of the Gulf of Mexico, which has 0 tidal amplitude for the M_2 constituent. This means that tidal characteristics for most stations in the study area have the unique characteristic of being mainly diurnal due to the proportionally larger K_1 and O_1 compared to the M_2 and S_2 harmonic constituents. This can be seen clearly in Figure 6-1, as the entrance to Brazos Santiago Pass (STX1820) demonstrates a classic diurnal tidal current signal of 1 large tidal pulse per day (Defant ratio = 3.68).

Stations in this study were positioned, when possible, to maximize the rectilinear flow of the currents, i.e., measure the back-and-forth tidal motion between flood and ebb to minimize any rotary characteristics. Of the 19 stations analyzed, 6 stations exhibited flow that is weak and variable or non-tidal; these stations are represented as “No Predictions” in Figure 6-1. This is fairly common due to the amphidromic point, which establishes flows in estuaries along the Texas coast are dominated by river or wind forcings. This low energy environment is confirmed by tidal ranges in Corpus Christi Bay and Laguna Madre that are usually no more than 0.33 m (<1 ft). For these 6 stations, additional rotary analyses were calculated, and only GI values were published in the Tidal Current Tables (TCTs) as subordinate stations. Predictions are available on the CO-OPS Tides and Currents website (NOAA, 2021a).

The analysis of 12 survey stations produced constituents which are available as TCP. Most stations show the amplitude of the diurnal constituents (Defant ratios) to be 2.5-5 times greater than the semidiurnal constituents, some with speeds up to 4 kn (200 cm/s). Figure 6-1 shows the Defant ratios for the study area.

The spatial distribution of the tidal ellipses of the principal semidiurnal (S_2 and M_2) and diurnal (K_1 and O_1) constituents are shown in Figures 6-2 through 6-5. The figures show that K_1 and O_1 are the dominant constituents, and that bathymetry (particularly the locations of channels) is the driving force behind the relative strength and orientation of the constituents, as well as the degree of rectilinearity of the ellipses.

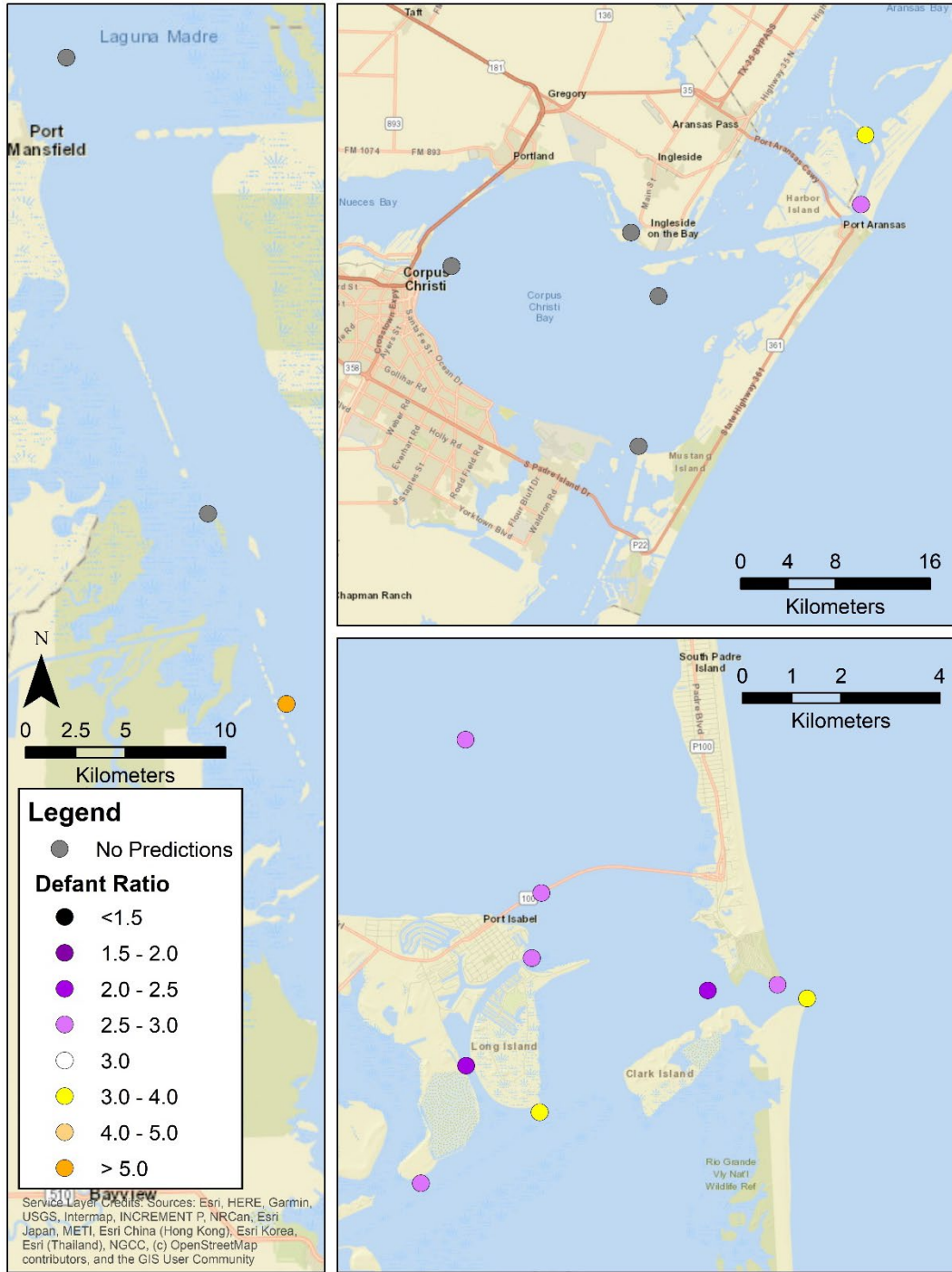


Figure 6-1. Defant ratios for survey stations. Neither strict semidiurnal tides (Defant ratio < 0.25) nor mixed-mainly semidiurnal tides (0.25 to 1.5) were found in the study area. Mixed mainly diurnal tides (> 1.5 to < 3.0) dominate in the lower Laguna Madre. The entrance to Corpus Christi had both mixed- mainly diurnal and predominately diurnal stations (Defant ratio > 3.0).

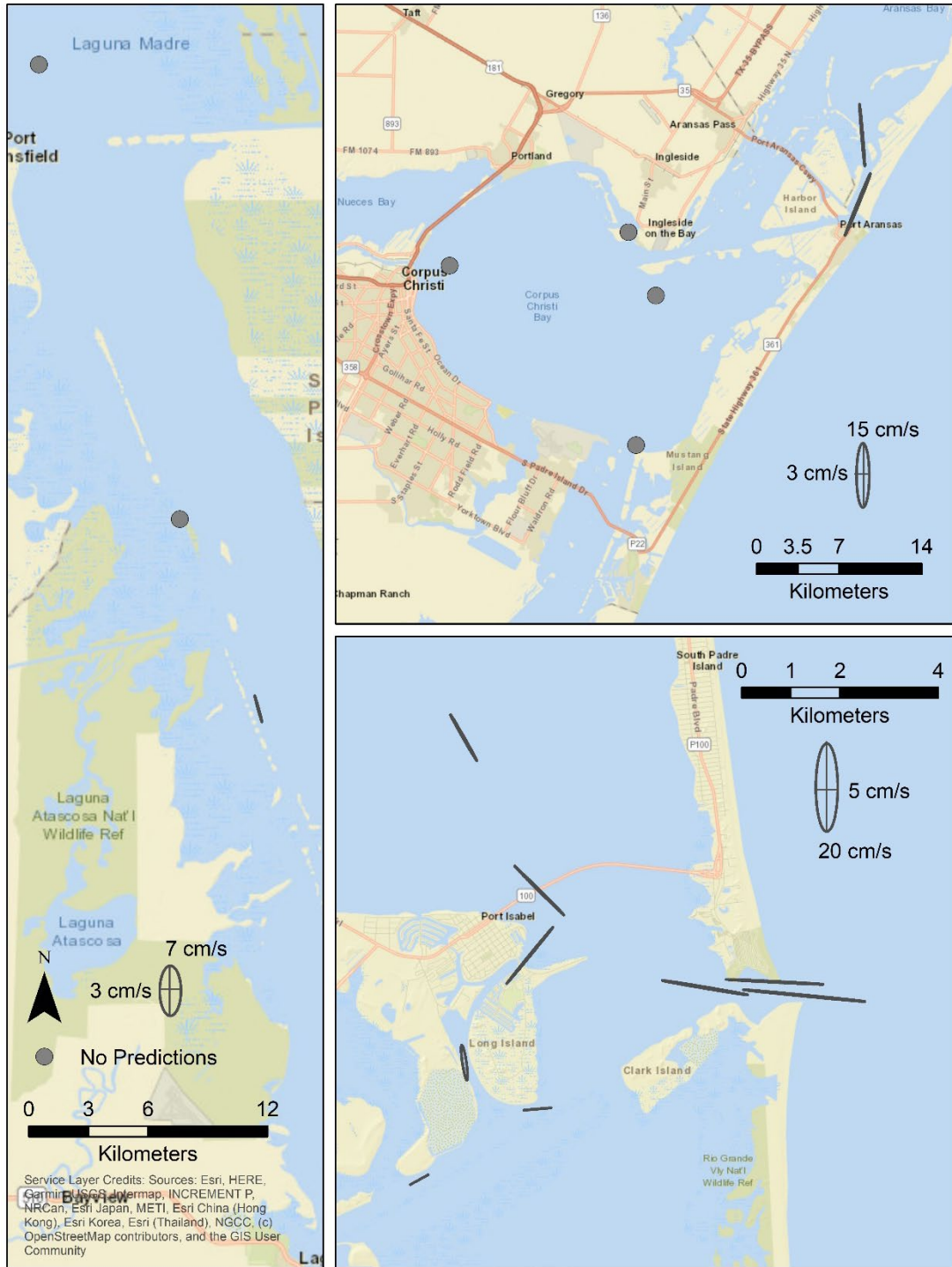


Figure 6-2. M₂ Tidal ellipses for prediction stations in the entire study region, showing the topographic steering of the ellipses.

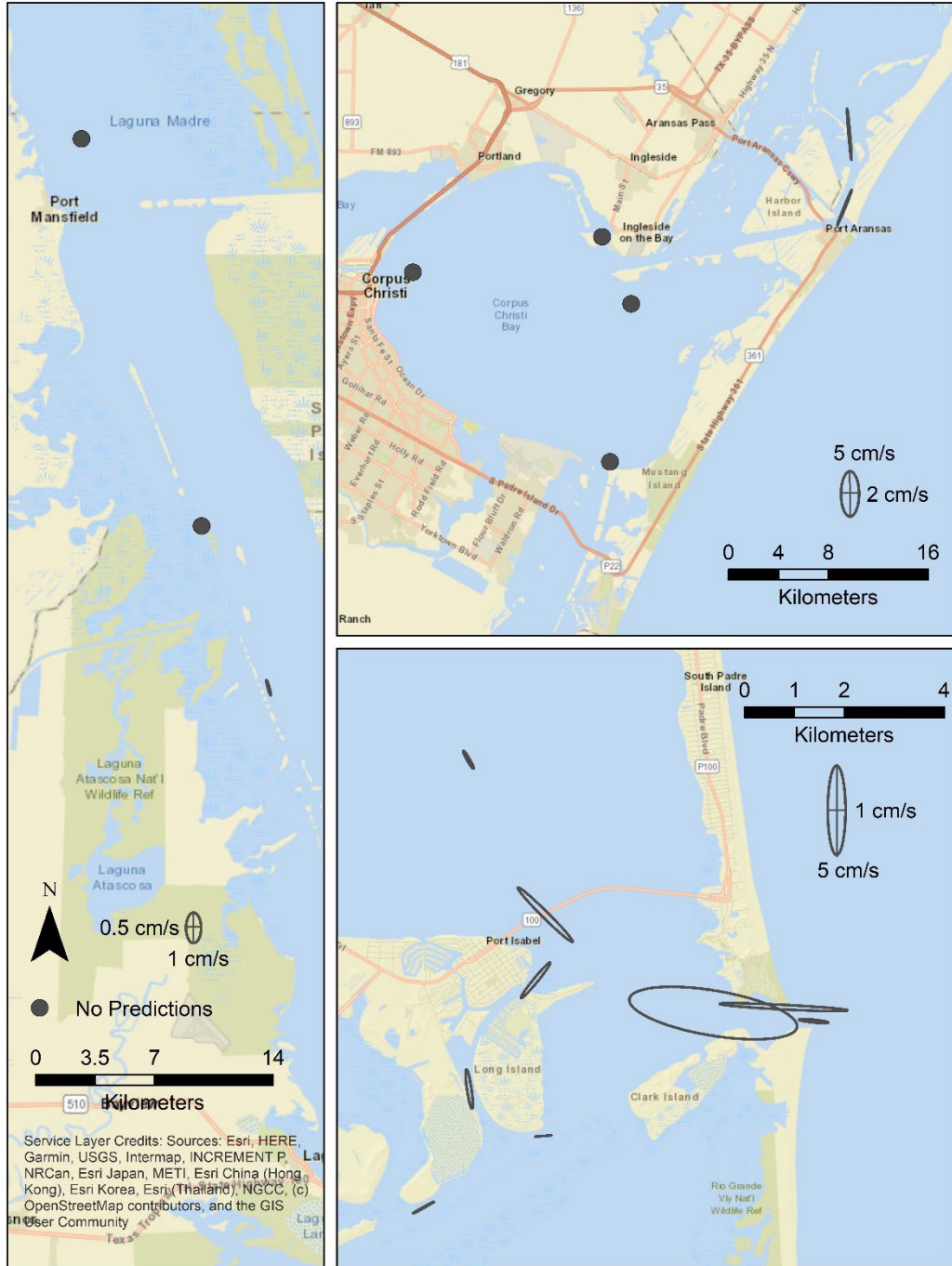


Figure 6-3. S_2 tidal ellipses for prediction stations in the entire study region. Note that these are on a different scale than M_2 in order to see the ellipses. These data are at a different scale than the M_2 data.

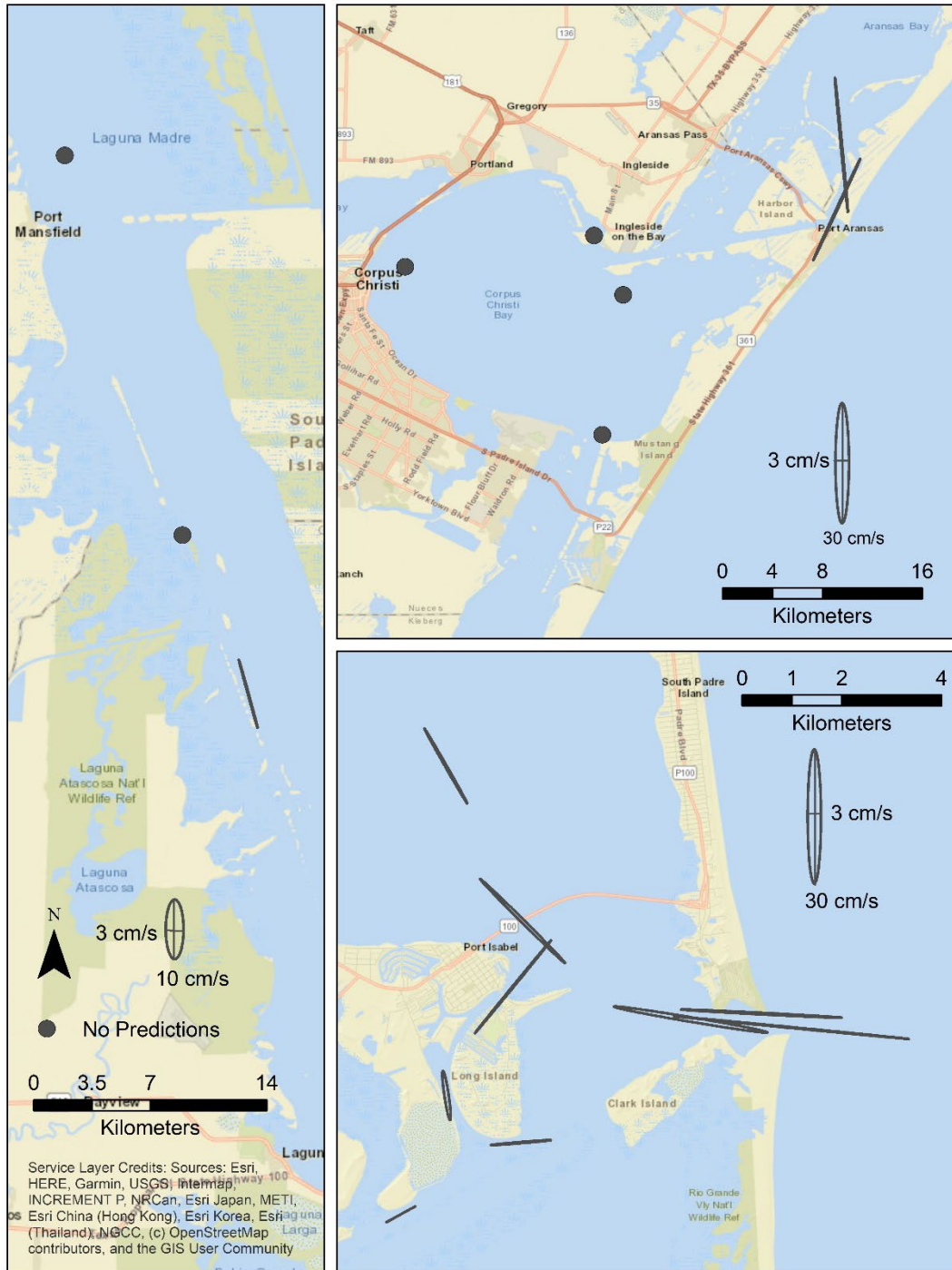


Figure 6-4. O₁ tidal ellipses for prediction stations in the entire study region. Note that these are on a different scale than M₂ in order to see the ellipses. These data are at a different scale than the M₂ data.

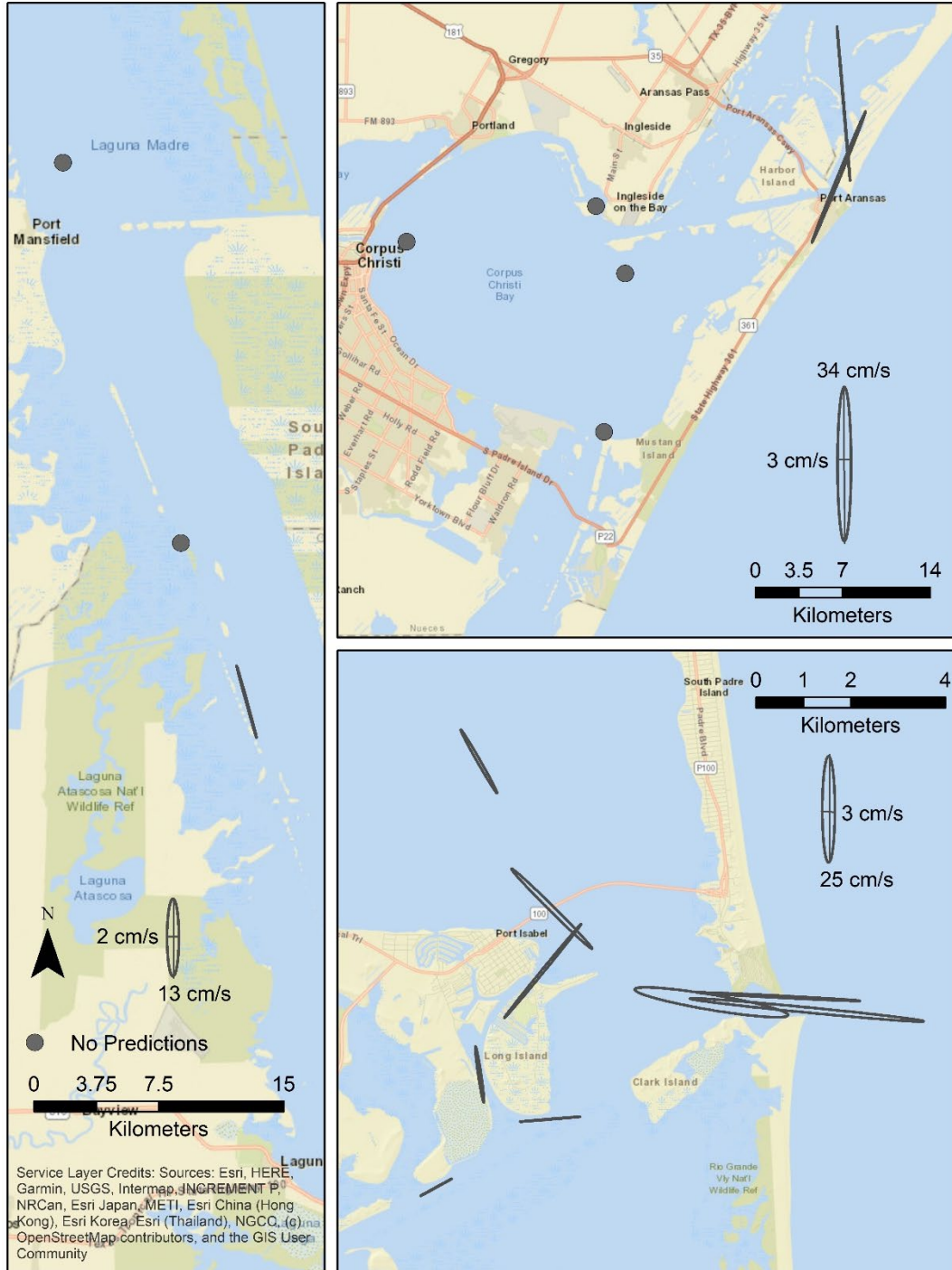


Figure 6-5. K_1 tidal ellipses for the entire study region. Note that these are on a different scale than M_2 in order to see the ellipses. These data are at $\frac{1}{4}$ the scale of the M_2 data.

6.2. Near-surface flows of the tidal current (timing and speed)

Maps of the magnitude and timing of mean ebb and flood currents show the movement of the tides within the estuary and how the amplitude changes due to bathymetry. Figure 6-6 shows the spatial distribution of the mean current magnitude and direction at each station during flood and ebb currents.

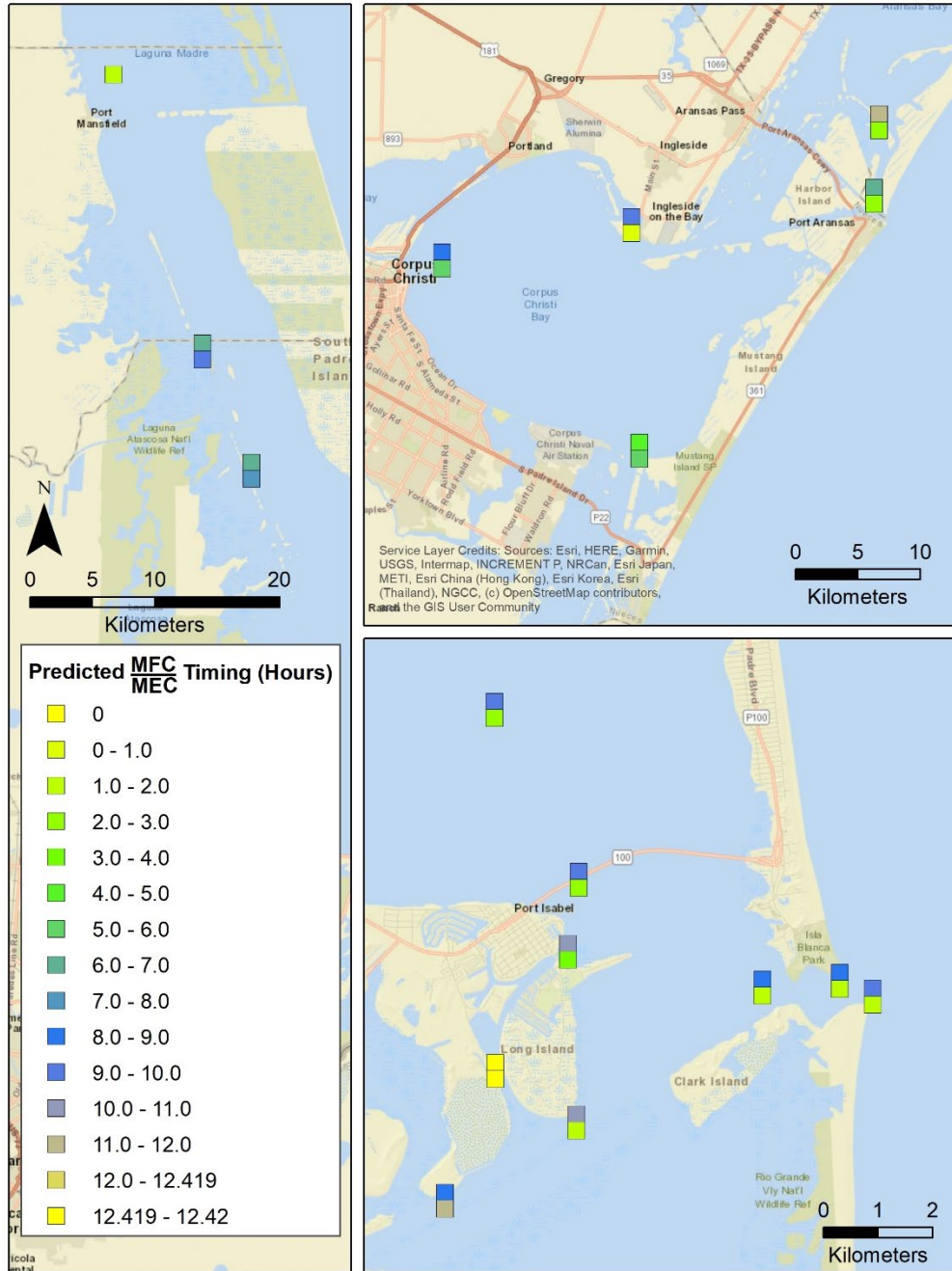


Figure 6-7. GI timing of maximum flood (top) and ebb (bottom) at all stations in the survey. Note that the colors represent hours from 0 to 12.42 with the end interval limits having the same colors to represent the cyclical tides.

7. SUMMARY

CO-OPS occupied 22 stations from 2017–2019 throughout the inland waters of the southwestern Gulf Coast of Texas. In addition to the current data obtained by the ADCPs, CTD profiles were collected during deployment and recovery of the ADCP at each station.

This current survey resulted in a multi-year data set of currents, water temperature, salinity, and pressure observations. The analysis showed that of the tidally-dominant stations in the region, most are mixed, mainly diurnal to diurnal. The tidal currents data were used to update NOAA tidal current predictions, which help to ensure safe and efficient navigation by improving the accuracy of observations and providing a higher density of predictions in the region.

All analyses and plots for the entire time series at all depths are available in detailed station reports (NOAA, 2021b). Updated tidal current predictions for each station are also available online via the CO-OPS Tides and Currents website (NOAA, 2021a). This data set is available to the public and research community by contacting CO-OPS' Stakeholder Services Branch at tide.predictions@noaa.gov to further investigate the circulation of this region and support safe and efficient navigation operations.

8. ACKNOWLEDGMENTS

We would like to thank Eddie Roggenstein, who was the CO-OPS Field Lead throughout the project, as well as the Atlantic Operations Branch who supported field operations; Katerina Glebushko for her oversight in the processing of data; and all the CO-OPS technicians, engineers, physical scientists, analysts, and oceanographers who assisted in station planning, the preparation of equipment, in field operations, and in the processing and dissemination of the data. Special thanks to Helen Worthington for initial manuscript editing and Virginia Dentler for final publishing.

9. REFERENCES

- Bosley, K.T., C McGrath, J. P. Dussault, M. Bushnell, M. J. Evans, G. W. French, and K. Earwaker (2005). Test, Evaluation, and Implementation of Current Measurement Systems on Aids-To-Navigation. NOAA Technical Report NOS CO-OPS 043.
- Defant, Albert (1958), Ebb and Flow the Tides of Earth, Air and Water. University of Michigan Press. Ann Arbor.
- Fanelli, P, C. Paternostro, G. Dusek, C. Kammerer, J. Park, and A. Carisio (2014), Potential Location Assessment of Coastal and Estuarine Surveys (PLACES). NOAA CO-OPS-NCOP.
- Gill, S.K., J.R. Hubbard, G. Dingle (1995), Tidal Characteristics and Datums of the Laguna Madre, Texas. NOAA Technical Memorandum NOS OES 008.
- Lanerolle, L.W., R.C. Patchen, and F. Aikman (2011), The second-generation Chesapeake Bay Operational Forecast System (CBOFS₂) Model Development and Skill Assessment: Technical Report, NOAA Technical Report, NOS CS 29.
- NOAA (2003). Computational Techniques for Tidal Datums, NOAA Special Publication NOS CO-OPS 2. Retrieved from: https://tidesandcurrents.noaa.gov/publications/Computational_Techniques_for_Tidal_Datums_handbook.pdf
- NOAA NOS Center for Operational Oceanographic Products and Services. (2021a). Retrieved from: <https://tidesandcurrents.noaa.gov/oaacurrents/Regions>
- NOAA NOS Center for Operational Oceanographic Products and Services, User Services. (2021b). Retrieved from: <https://tidesandcurrents.noaa.gov/contact.html>
- NOAA NOS Center for Operational Oceanographic Products and Services. (2021c). Retrieved from: <https://tidesandcurrents.noaa.gov/stations.html?type=Datums>
- NOAA (2021d), U.S. Coast Pilot5, Gulf of Mexico, Puerto Rico and Virgin Islands, 49th Edition. U.S. Department of Commerce, National Oceanic and Atmospheric Administration, National Ocean Service.
- NOAA (2018), NOAA's Contribution to the Economy; Powering America's Economy and Protecting Americans. <http://performance.noaa.gov/economics>
- Parker, B.B. (2007). Tidal Analysis and Prediction. Silver Spring, MD: Center for Operational Oceanographic Products and Services, National Ocean Service, NOAA. Library of Congress Control Number: 2007925298.

- Paternostro, C.L., A. Pruessner, and R. Semkiw (2005), Designing a Quality Oceanographic Data Processing Environment. MTS/IEEE Oceans Conference. Washington, D.C.
- Schoenbaechler, C., C.G. Guthrie, J. Matsumoto, Q. Lu, and S. Negusse (2011a), TxBLEND Model Calibration and Validation for the Nueces Estuary. Texas Water Development Board, Austin, Texas.
- Schoenbaechler, C., C.G. Guthrie, J. Matsumoto, and Q. Lu. (2011b), TxBLEND Model Calibration and Validation for the Laguna Madre Estuary. Texas Water Development Board, Austin, Texas.
- Swanson, R.L. (1974), Variability of Tidal Datums and Accuracy in Determining Datums from Short Series of Observations, NOAA Technical Report 64. Rockville, MD: NOAA U.S. Department of Commerce
- Texas Water Development Board (2021a), Nueces Estuary (Corpus Christi Bay). Retrieved from: https://www.twdb.texas.gov/surfacewater/bays/major_estuaries
- Texas Water Development Board (2021b), Laguna Madre Estuary. Retrieved from: https://www.twdb.texas.gov/surfacewater/bays/major_estuaries/laguna_madre/index.asp
- U.S. Integrated Ocean Observing System, (2019). QARTOD. Manual for Real-Time Quality Control of In-Situ Current Observations Version 2.1: A Guide to Quality Control and Quality Assurance of Acoustic Doppler Current Profiler Observations. 52 pp. <https://doi.org/10.25923/sqe9-e310>
- U.S. Integrated Ocean Observing System, (2020). QARTOD. Manual for Real-Time Oceanographic Data Quality Control Flags Version 1.2. https://cdn.ioos.noaa.gov/media/2020/07/QARTOD-Data-Flags-Manual_version1.2final.pdf
- U.S. Coast Guard (2016), Use of Electronic Charts and Publications in Lieu of Paper Charts, Maps and Publications. COMDTPUB P16700.4 Navigation and Vessel Inspection Circular 01-16, Washington D.C., U.S. Department of Homeland Security
- Zervas, C. (1999), Tidal Current Analysis Procedures and Associated Computer Programs. NOAA Technical Memorandum NOS CO-OPS 0021, Silver Spring, MD: NOAA, U.S. Department of Commerce

APPENDIX A, STATION LISTING

Table A-1. Station location and deployment information. Stations not recovered (italicized) do not have a recovery date.

Station ID	Station Name	Latitude	Longitude	Depth (m)	Deployment	Recovery
STX1801	Lydia Ann Channel, S end	27.85261	-97.0548	4.5	12/1/2018	1/30/2019
STX1802	Murray Shoal	27.89929	-97.05143	4	12/1/2018	1/30/2019
STX1803	La Quinta Channel	27.83392	-97.22953	14.1	12/1/2018	1/31/2019
STX1804	Corpus Christi Channel (moved)	27.81131	-97.36578	5.4	12/1/2018	1/31/2019
<i>STX1805</i>	<i>ICW - CC Bay Northern Ent</i>	<i>27.81196</i>	<i>97.19558</i>	<i>3</i>	<i>12/1/2018</i>	
STX1806	ICW - CC Bay Light 51	27.79111	-97.20854	3.8	12/1/2018	1/31/2019
STX1807	ICW - CC Bay Southern Ent	27.69031	-97.22362	2.4	12/1/2018	2/1/2019
STX1808	ICW Port Mansfield, 2 nm N of	26.53386	-97.40228	3	5/5/2018	8/7/2018
<i>STX1809</i>	<i>ICW Port Mansfield, 1.5 NM S of</i>	<i>26.53386</i>	<i>-97.40228</i>	<i>2.5</i>	<i>5/5/2018</i>	
<i>STX1810</i>	<i>Port Mansfield Channel Entrance</i>	<i>26.56398</i>	<i>-97.27631</i>	<i>5.1</i>	<i>11/30/2017</i>	
STX1811	ICW at Arroyo Colorado	26.40459	-97.34506	4	2/3/2018	5/2/2018
STX1812	ICW Laguna Madre, 2.25 nm S of Arroyo Colorado Cutoff	26.32787	-97.30972	3.5	2/3/2018	5/2/2018
STX1813	ICW Light 69	26.10755	-97.2116	3.5	12/1/2017	1/31/2018
STX1814	Queen Isabella Causeway Bridge	26.08127	-97.2117	5.5	5/4/2018	12/4/2018
STX1815	Port Isabel, Pontoon Swing Bridge	26.07183	-97.19948	5.5	12/1/2017	1/30/2018
STX1816	Port Isabel Channel	26.05521	-97.21236	6	11/17/2017	2/1/2019
STX1817	Brownsville Ship Channel, east end	26.03497	-97.21973	8.5	12/1/2017	1/30/2018
STX1818	Laguna Madre Channel, SW end	26.04664	-97.1981	6	12/1/2017	1/30/2018
STX1819	Laguna Madre Channel, NE end	26.06652	-97.16755	7.4	8/8/2018	12/4/2018
STX1820	Brazos Santiago Pass Entrance	26.06518	-97.14944	13.5	12/1/2017	1/31/2018
STX1821	Brazos Santiago Pass (SPIP)	26.06746	-97.15481	5	11/21/2017	2/4/2019
STX1822	Port Isabel Channel, damaged pier	26.05421	-97.21146	8.6	5/4/2018	8/9/2018

APPENDIX A. STATION PLATFORM TYPES

Table B- 1. Platform and sensor information for recovered stations, including first bin distance and number of good bins.

Station ID	Mount type	ADCP Type	First Bin Distance	Bin Size	No. of Good Bins
STX1801	Tripod	WHADCP 1200 kHz	1.1	0.5	6
STX1802	Fiberglass grate	Nortek-2MHz	0.7	0.5	6
STX1803	GP35	WHADCP 600 kHz	2.1	1	11
STX1804	Tripod	Nortek-1MHz	1.5	1	4
STX1806	Tripod	WHADCP 1200 kHz	1.1	0.5	4
STX1807	Fiberglass Grate	Nortek-2MHz	0.7	0.5	3
STX1808	Fiberglass grate	Nortek-2MHz	0.7	0.5	5
STX1811	Fiberglass grate	Nortek-2MHz	0.7	0.5	5
STX1812	Fiberglass Grate	Nortek-2MHz	0.7	0.5	3
STX1813	Fiberglass grate	Nortek-2MHz	0.7	0.5	3
STX1814	Custom SL Clamp	Nortek - Z Cell	2.5	2	16
STX1815	Tripod	WHADCP 1200 kHz	1.1	0.5	8
STX1817	Tripod	WHADCP 1200 kHz	1.5	1	6
STX1818	Tripod	WHADCP 1200 kHz	1.5	1	4
STX1819	ATON	Nortek-1MHz	0.9	0.5	9
STX1820	GP35	WHADCP 600 kHz	2.1	1	9
STX1821	SPIP	Nortek AWAC	5.0	4	30
STX1822	Pier piling	Nortek-1MHz	2.5	2	18

ACRONYMS

ADCP	acoustic Doppler current profiler
AIS	Automatic identification system
AqD	Nortek Aquadopp current meter
ATON	Aids to Navigation
AWAC	acoustic wave and current profiler manufactured by Nortek
C	Celsius
cm/s	Centimeters per second
CO-OPS	Center for Operational Oceanographic Products and Services
CTD	conductivity-temperature-depth
CFR	Code of Federal Regulations
ENU	Instrument orientation relative to the Earth: East, North, and Up
ft	feet
GI	Greenwich Interval
GIWW	Gulf Intracoastal Waterway
GP35	General Purpose 35-inch bottom mount platform from Mooring Systems, Inc. This platform has been renamed as H-TRBM-35 by the manufacturer.
Gt	Great diurnal range (MHHW-MLLW)
H-TRBM	Hemispheric Trawl-resistant bottom mount
ICW	Intracoastal Waterway
IHO	International Hydrographic Organization
kg	kilogram
kHz	kilohertz
km	kilometer
kn	knots
LSQHA	Least squares harmonic analysis
m	meter
MEC	maximum ebb current
MFC	maximum flood current
MHz	megahertz
MHHW	mean higher high water
MLLW	mean lower low water
MSI	Mooring Systems, Inc.
MTRBM	miniature trawl-resistant bottom mount
NCOP	National Current Observation Program
nmi	nautical mile
NOAA	National Oceanic and Atmospheric Administration
NOS	National Ocean Service
NWLON	National Water Level Observation Network
PORTS®	Physical Oceanographic Real-Time System
QARTOD	Quality Assurance/Quality Control of Real-Time Oceanographic Data
QC	Quality control
R/V	Research Vessel
s	second
SPIP	Single Pile Instrumentation Platform

STX	Southwest Texas
TCP	Tidal Current Predictions
TCTs	(published) Tidal Current Tables
TRBM	trawl-resistant bottom mount
TRDI	Teledyne RD Instruments
USC	United States Code
XYZ	Instrument orientation relative an instrument's X-Axis, Y-Axis, and Z-Axis